Geophys. J. Int. (2012) **189,** 1597–1610 doi: 10.1111/j.1365-246X.2012.05430.x

Two-point paraxial traveltimes in an inhomogeneous anisotropic medium

Vlastislav Červený,[1] Einar Iversen[2] and Ivan Pšenčík[3]

[1]*Faculty of Mathematics and Physics, Department of Geophysics, Charles University in Prague, Ke Karlovu* 3, 121 16 *Praha* 2*, Czech Republic. E-mail: vcerveny@seis.karlov.mff.cuni.cz*

[2]*Norsar,* P.O. Box 53, 2027 *Kjeller, Norway. E-mail: Einar.Iversen@norsar.no*

[3]*Institute of Geophysics, The Academy of Sciences of Czech Republic, Boční II,* 141 31 *Praha* 4*, Czech Republic. E-mail: ip@ig.cas.cz*

Accepted 2012 February 22. Received 2012 February 21; in original form 2011 November 8

SUMMARY

We derive formulae for the approximate computation of two-point paraxial traveltimes (traveltimes between two points) for points arbitrarily chosen in a paraxial vicinity of a reference ray computed in a smoothly varying inhomogeneous anisotropic medium containing structural interfaces. The formulae have a form of the Taylor expansion in Cartesian coordinates of the two-point paraxial traveltime or its square to the quadratic terms. The coefficients of the expansion depend on quantities obtained by ray tracing in Cartesian coordinates and by dynamic ray tracing in ray-centred coordinates. Alternatively, the dynamic ray tracing can be performed in Cartesian coordinates. The advantages of the approach based on dynamic ray tracing in ray-centred coordinates are its efficiency and elimination of possible complications that may arise from the redundant fundamental solutions of dynamic ray tracing in Cartesian coordinates (the ray-tangent and non-eikonal solutions). As a by-product, we also obtain simple formulae for the slowness vectors at the two points in the paraxial vicinity of the reference ray. They belong to a paraxial ray passing through these points. Potential applications of the proposed formulae consist in the fast and flexible two-point traveltime calculations from sources to receivers specified in Cartesian coordinates and situated close to a reference ray, along which dynamic ray tracing has been performed. The formulae for the paraxial slowness vectors can be used in two-point ray tracing.

Key words: Body waves; Seismic anisotropy; Theoretical seismology; Wave propagation.

1 INTRODUCTION

We consider a smoothly varying inhomogeneous anisotropic medium containing smooth structural interfaces. In it, we compute a reference ray Ω, and select two arbitrarily situated points S and R on it. Along the ray, we determine the 4×4 ray propagator matrix in ray-centred coordinates, initialized as the 4×4 identity matrix $\mathbf{I}$ at S. We assume that conditions of applicability of the ray method are satisfied.

We choose a point S' in a 3-D vicinity of S, and a point R' in a 3-D vicinity of R, and specify the position of the points S' and R' in Cartesian coordinates. Our goal is to determine approximately the two-point traveltime $T(R', S')$ from S' to R' and the slowness vectors $\mathbf{p}(S')$ and $\mathbf{p}(R')$ corresponding to the ray connecting S' and R'. The standard ray method can be used to compute the traveltime and the slowness vector (gradient of the traveltime field) only along the ray Ω (containing points R and S), not in its vicinity (at points R' and S'). In the vicinity of the ray Ω, however, we can use the extension of the ray method, called the 'paraxial ray method' (Červený 2001, chapter 4; Moser & Červený 2007). In principle, the paraxial ray method is based on the Taylor expansion of the traveltime from the reference ray Ω to its vicinity, up to the second-order terms. The second-order coefficients of the Taylor expansion can be determined using the ray propagator matrix, computed along the reference ray Ω by dynamic ray tracing. We therefore speak of two-point 'paraxial' traveltime $T(R', S')$, and 'paraxial' slowness vector $\mathbf{p}(R')$ and $\mathbf{p}(S')$. We emphasize that these quantities are determined without performing ray tracing between S' and R'. We use solely the quantities determined by tracing the reference ray Ω between S and R, and by dynamic ray tracing along Ω. The two-point traveltime is then expanded in Cartesian coordinates only in a 3-D vicinity of S and R.

All expressions derived in this paper are very general and flexible, as they allow to consider points S' and R' arbitrarily situated in the quadratic (paraxial) vicinity of S and R, not only on some specific surfaces (anterior, posterior, tangential to the wavefront at Ω, perpendicular to the ray Ω, etc.). The expressions are specified in Cartesian coordinates, their coefficients are, however, evaluated by dynamic ray tracing in ray-centred coordinates. This makes the proposed approach efficient and free of possible complications that may arise from the redundant fundamental solutions of dynamic ray tracing (the ray-tangent and non-eikonal solutions). This represents an extension of existing approaches.

The two-point paraxial traveltime $T(R', S')$ is an approximation of the traveltime along the paraxial ray $\Omega'(R', S')$, passing through the points S' and R'. If the paraxial ray $\Omega'(R', S')$ is known, the traveltime $T(R', S')$ can be calculated easily, by quadratures along Ω'. An extensive literature is devoted to the two-point ray tracing, particularly in inhomogeneous isotropic layered structures. Various approaches have been used in this field, see for example, Bulant (1996, 1999), Grechka & McMechan (1996) and a detailed review in Červený (2001, section 3.11). Here, we study only the two-point 'paraxial' traveltimes.

The interest in the two-point paraxial traveltime $T(R', S')$ has a long tradition. It has been discussed already by Hamilton in the first half of the nineteenth century (Hamilton 1837). It is well known that Hamilton derived equations for geodesics, which represent equations for rays. Therefore, the ray equations are sometimes called Hamilton's equations at present. Hamilton, however, also studied the traveltime between two points, and called it 'the characteristic function'. To acknowledge Hamilton's contribution to this field, the characteristic function is now also called 'Hamilton's characteristic function'. For more detailed explanations and discussions of Hamilton's work in this field see Klimeš (2009). Klimeš also extended Hamilton's treatment of the characteristic function by the equations of geodesic deviations in Cartesian coordinates (in seismic literature and also in this paper called the dynamic ray tracing equations) and derived the relations between the 6×6 ray propagator matrix of dynamic ray tracing in Cartesian coordinates and the second-order spatial derivatives of the Hamilton's characteristic function. The second-order spatial derivatives of the characteristic function can be used to compute the two-point paraxial traveltime $T(R', S')$, with the second-order accuracy in terms of the distances $S' - S$ and $R' - R$. The approach requires to compute the 6×6 ray propagator matrix in Cartesian coordinates. In this paper, however, we use mostly the 4×4 ray propagator matrix in ray-centred coordinates, supplemented by transformation equations to Cartesian coordinates at points S and R, to compute $T(R', S')$. Only in Section 5, we discuss briefly an alternative approach based on the direct use of 6×6 ray propagator matrices in Cartesian coordinates.

For isotropic inhomogeneous media, the equation for the two-point paraxial traveltime $T(R', S')$ between points S' and R' specified in Cartesian coordinates, was first presented by Červený *et al.* (1984). The points S' and R' were situated in a paraxial vicinity of the reference ray Ω, along which the dynamic ray tracing in ray-centred coordinates was performed and the 4×4 ray propagator matrix in ray-centred coordinates was determined. See also Červený (2001, eq. 4.9.24), where the derivation is given in a greater detail.

Closely related methods based on paraxial approximation of traveltime have been used in the theory of optical systems (e.g. Luneburg 1964), and in analogous theory of seismic systems (e.g. Bortfeld 1989; Hubral *et al.* 1992). The applications in optics and seismic exploration are, however, different. In optics, where the function $T(R', S')$ is often called the two-point eikonal, the theory of optical systems is used primarily in the design of optical instruments. In seismology, the seismic systems represent the geological structures of the Earth explored by seismic waves. See also the surface-to-surface formalism, in which the points S and S' are situated close to each other on some anterior surface, and points R and R' close to each other on some posterior surface (Hubral *et al.* 1992; Schleicher *et al.* 1993; Červený 2001; Červený & Moser 2007). The method presented here represents an extension of the surface-to-surface formalism, in which the points S' and R' are also situated close to points S and R, respectively, but in a 3-D paraxial vicinity of S and R. No anterior and posterior surfaces are considered. The positions of points S', R', S and R are specified in global Cartesian coordinates.

The two-point paraxial traveltime $T(R', S')$ may be used in many applications in seismology and seismic exploration; practically in all situations, where the traveltime of seismic waves plays an important role. It may be used when only a single reference ray is considered. From the equation for $T(R', S')$, we can also simply determine the Taylor series for $T^2(R', S')$ up to the quadratic terms. The latter is exact for an isotropic homogeneous medium. Thus, it is expected that the use of expressions for traveltime squared in weakly inhomogeneous media, either isotropic or weakly anisotropic, may provide highly accurate results. The formulae for two-point paraxial traveltime and its square have useful applications in seismic prospecting and seismology. As examples we mention seismic depth migration and velocity analysis (Gjøystdal *et al.* 1984; Buske *et al.* 2009), the common-reflection surface (CRS) method (Hubral *et al.* 1998), Kirchhoff modelling and migration (e.g. Gjøystdal *et al.* 2007; Alkhalifah & Fomel 2010), common-angle migration (Brandsberg-Dahl *et al.* 2003), Fresnel-volume modelling (Červený & Soares 1992) and microearthquake location (Gharti *et al.* 2010). A certain disadvantage is that the method is based on extrapolation of the traveltime from a reference ray Ω so that its accuracy is lower in regions where the structure is strongly varying.

Briefly to the content of the paper. As the non-orthogonal ray-centred coordinates are used broadly in the paper, Section 2 is used to introduce their covariant and contravariant basis vectors and the 4×4 ray propagator matrix in this coordinate system. Ray tracing and dynamic ray tracing equations, however, are not presented here, as they are well described in the referred literature. In Section 3, we show how the 4×4 ray propagator matrix in ray-centred coordinates can be used to compute the second derivatives of the paraxial traveltimes with respect to ray-centred coordinates and the two-point paraxial traveltimes $T(R', S')$, with points R' and S' situated in planes tangent to the wavefront at R and S, respectively. A useful formula for $T^2(R', S')$ is also given. In Section 4, we explain how the second derivatives of two-point paraxial traveltimes with respect to ray-centred coordinates can be transformed to second derivatives of two-point paraxial traveltimes with respect to Cartesian coordinates. Section 4 also contains final equations for the two-point paraxial traveltime $T(R', S')$, where the paraxial points S' and R' are specified in Cartesian coordinates, with points S and R situated on the reference ray Ω. We emphasize here that the points S', R', S and R are specified in general Cartesian coordinates, but the dynamic ray tracing is performed in ray-centred coordinates, and the 4×4 ray propagator matrix is also computed in ray-centred coordinates. In this section, we also give the expressions for slowness vectors at S' and R' and the formula for $T^2(R', S')$ in the vicinity of the reference ray Ω. In Section 5, we derive an alternative form of a two-point paraxial traveltime $T(R', S')$ in Cartesian coordinates, in which the dynamic ray tracing is used directly in Cartesian coordinates and the 6×6 propagator matrix in Cartesian coordinates is computed. In Section 6, we mention some special cases, and in Section 7 we discuss possible applications in seismic exploration and seismology. Finally, in Section 8 we offer some concluding remarks.

In the whole paper, we tacitly assume that the medium, in which the reference ray Ω is situated, is 3-D, inhomogeneous, anisotropic and perfectly elastic. The medium may also contain structural interfaces. In this case, of course, ray tracing and dynamic ray tracing procedures must take the structural interfaces into account. Such procedures are, however, now available in existing literature and are

not discussed here. See, for example, Farra & LeBégat (1995) and Červený & Moser (2007). It is assumed that the points S and S' are situated in the same layer (block). The same assumption is made on points R and R'. For the sake of brevity, we call sometimes points S' and R', situated in paraxial vicinities of S and R, respectively, the paraxial points.

We use both the componental and matrix notations in the paper. In the componental notation, the upper-case indices (I, J, K, ...) take the values 1 and 2, and the lower-case indices (i, j, k, ...) the values 1, 2 or 3. The Einstein summation convention is used. In the matrix notation, the matrices and vectors are denoted by bold upright symbols. The vectors are represented by column matrices, either 3×1 or 2×1. The scalar product of vectors $\mathbf{a}$ and $\mathbf{b}$ reads $\mathbf{a}^T\mathbf{b}$, the dyadics reads $\mathbf{a}\mathbf{b}^T$, where the superscript T denotes the transpose. In matrix notation, we also use notation $\mathbf{A}^{-1}$ for the inverse of matrix $\mathbf{A}$, and $\mathbf{A}^{-T}$ for the transpose of the inverse of matrix $\mathbf{A}$. The dimensions of matrices are mostly explained in the text in places where the matrices are used.

2 RAY TRACING AND DYNAMIC RAY TRACING

Here we briefly describe quantities needed in the computation of paraxial slowness vectors and two-point paraxial traveltimes in anisotropic inhomogeneous media. These quantities are obtained by ray tracing of the reference ray Ω and by dynamic ray tracing along the reference ray. Ray tracing and dynamic ray tracing are well described in seismological literature, and are not discussed here. For anisotropic inhomogeneous media, see, for example, Babich (1961), Červený (1972), Gajewski & Pšenčík (1987, 1990), Farra & Madariaga (1987), Klimeš (1994), Farra & Le Bégat (1995), Chapman (2004), Iversen (2004), Klimeš (2006b) and Červený *et al.* (2007). Particularly detailed treatment, including additional literature, can be found in Červený (2001). In this section, we only introduce and define the quantities needed in the following sections.

2.1 Quantities computed by ray tracing

We consider the eikonal equation in the Hamiltonian form

$$\mathcal{H}(x_i, p_j) = \tfrac{1}{2}. \tag{1}$$

The Hamiltonian $\mathcal{H}$ is a function of Cartesian coordinates x_i and of the Cartesian components p_j of the slowness vector $\mathbf{p}$. We assume that $\mathcal{H}(x_i, p_j)$ is a homogeneous function of the second degree in p_j. In this case, the parameter τ along a ray Ω corresponding to this Hamiltonian is a traveltime. The slowness vector $\mathbf{p}(\tau)$ is perpendicular to the wavefront at any point of Ω. The reference ray Ω is specified by the initial conditions x_i^0 and p_i^0 at an initial point. On the ray Ω, we select two arbitrarily situated points S and R.

At any point along the ray Ω, specified by parameter τ, ray tracing yields the Cartesian coordinates $x_i(\tau)$ of that point, and the quantities $p_i(\tau)$, $\mathcal{U}_i(\tau)$ and $\eta_i(\tau)$, which are the Cartesian components of the slowness vector $\mathbf{p}(\tau)$, ray-velocity vector $\boldsymbol{\mathcal{U}}(\tau) = \mathrm{d}\mathbf{x}(\tau)/\mathrm{d}\tau$ and vector $\boldsymbol{\eta}(\tau) = \mathrm{d}\mathbf{p}(\tau)/\mathrm{d}\tau$, respectively. The slowness vector $\mathbf{p}$ satisfies the relation $\mathbf{p}^T(\tau)\,\boldsymbol{\mathcal{U}}(\tau) = 1$ at any point of Ω.

2.2 Ray-centred coordinate system

The non-orthogonal ray-centred coordinate system $\mathbf{q} \equiv (q_1, q_2, q_3 = \tau)$ is connected with the reference ray Ω. It is introduced by the following transformation relation with respect to Cartesian coordinates $\mathbf{x} \equiv (x_1, x_2, x_3)$:

$$x_i(q_j) = x_i(\tau) + H_{iM}(\tau) q_M \,. \tag{2}$$

The reference ray Ω is specified by eq. (2) for $q_M = 0$, and represents the τ-coordinate line, so that q_3 represents the time variable τ along the reference ray Ω. Coordinates q_1, q_2 are 2-D Cartesian coordinates which specify uniquely the position of a point in the plane Σ_τ perpendicular to the slowness vector of the reference ray Ω at a given time τ. In anisotropic media, the coordinate system q_1, q_2, q_3 is non-orthogonal, as the reference ray is not perpendicular to the plane Σ_τ. In isotropic media, the coordinate system q_1, q_2, q_3 is orthogonal, but not orthonormal. If we, however, consider only the two ray-centred coordinates q_1, q_2 in the plane Σ_τ, the 2-D Cartesian coordinate system q_1, q_2 in the plane Σ_τ is always orthonormal.

The 3×3 matrix $\mathbf{H}$ represents the transformation matrix from ray-centred q_m to Cartesian x_i coordinates,

$$H_{im} = \partial x_i / \partial q_m. \tag{3}$$

Columns of matrix $\mathbf{H}$ are contravariant basis vectors $\mathbf{e}_1$, $\mathbf{e}_2$, $\mathbf{e}_3$ of the ray-centred coordinate system

$$\mathbf{H} = (\mathbf{e}_1, \mathbf{e}_2, \mathbf{e}_3 = \boldsymbol{\mathcal{U}}) \,. \tag{4}$$

Consequently,

$$H_{iM} = \partial x_i / \partial q_M = e_{Mi}, \tag{5}$$

where e_{Mi} is the ith Cartesian component of the basis vector $\mathbf{e}_M$. The basis vectors $\mathbf{e}_1$, $\mathbf{e}_2$ may be introduced in several ways (Klimeš 2006a). Here we introduce them as two mutually perpendicular unit vectors, perpendicular to $\mathbf{p}$, and thus tangent to the wavefront at its intersection with the reference ray Ω. In anisotropic media, vectors $\mathbf{e}_1$ and $\mathbf{e}_2$ are not generally perpendicular to $\boldsymbol{\mathcal{U}}$. One of the basis vectors $\mathbf{e}_1$ and $\mathbf{e}_2$ can be determined by solving the ordinary differential equation (Klimeš 2006a, see also Červený *et al.* 2007)

$$\frac{\mathrm{d}\mathbf{e}_I}{\mathrm{d}\tau} = -(\mathbf{p}^T\mathbf{p})^{-1}\left(\mathbf{e}_I^T\boldsymbol{\eta}\right)\mathbf{p} \tag{6}$$

along the ray Ω. The other basis vector can then be calculated using the orthogonality of $\mathbf{e}_1$, $\mathbf{e}_2$ and $\mathbf{p}$. For example, when $\mathbf{e}_1$ is calculated using (6), $\mathbf{e}_2$ is obtained from the relation

$$\mathbf{e}_2 = \mathbf{p} \times \mathbf{e}_1 / |\mathbf{p} \times \mathbf{e}_1| \,. \tag{7}$$

It is useful to consider the 3×3 transformation matrix $\overline{\mathbf{H}}$ from Cartesian x_i to ray-centred coordinates q_m:

$$\overline{H}_{mi} = \partial q_m / \partial x_i \,. \tag{8}$$

The elements of 3×3 matrices $\mathbf{H}$ and $\overline{\mathbf{H}}$ satisfy the relation

$$\overline{H}_{mi} H_{in} = \delta_{mn}. \tag{9}$$

The matrices $\mathbf{H}$ and $\overline{\mathbf{H}}$ are inverses of each other. Rows of 3×3 matrix $\overline{\mathbf{H}}$ consist of covariant basis vectors $\mathbf{f}_1, \mathbf{f}_2, \mathbf{f}_3$ of the ray-centred coordinate system:

$$\overline{\mathbf{H}} \equiv (\mathbf{f}_1, \mathbf{f}_2, \mathbf{f}_3 = \mathbf{p})^T, \tag{10}$$

where

$$\overline{H}_{Mi} = \partial q_M / \partial x_i = f_{Mi}, \tag{11}$$

and f_{Mi} is the ith Cartesian component of the covariant basis vector $\mathbf{f}_M$. The covariant basis vectors $\mathbf{f}_m$ can be calculated simply from the contravariant basis vectors $\mathbf{e}_I$ and $\boldsymbol{\mathcal{U}}$ and $\mathbf{p}$ using the relations

$$\mathbf{f}_1 = \frac{\mathbf{e}_2 \times \boldsymbol{\mathcal{U}}}{\boldsymbol{\mathcal{U}}^T(\mathbf{e}_1 \times \mathbf{e}_2)} = \mathcal{C}^{-1}(\mathbf{e}_2 \times \boldsymbol{\mathcal{U}}) ,$$
$$\mathbf{f}_2 = \frac{\boldsymbol{\mathcal{U}} \times \mathbf{e}_1}{\boldsymbol{\mathcal{U}}^T(\mathbf{e}_1 \times \mathbf{e}_2)} = \mathcal{C}^{-1}(\boldsymbol{\mathcal{U}} \times \mathbf{e}_1) , \quad \mathbf{f}_3 = \mathbf{p} . \tag{12}$$

Here $\mathcal{C}$ is the phase velocity of the wave under consideration, $\mathcal{C} = 1/|\mathbf{p}|$. Thus, the contravariant basis vectors $\mathbf{e}_1, \mathbf{e}_2$ are perpendicular to the slowness vector $\mathbf{p}$, and the covariant basis vectors $\mathbf{f}_1, \mathbf{f}_2$ are perpendicular to the ray-velocity vector $\boldsymbol{\mathcal{U}}$ at any point of the ray Ω. Vectors $\mathbf{e}_i$ and $\mathbf{f}_i$ satisfy the relation

$$\mathbf{e}_i^T \mathbf{f}_j = \delta_{ij} \tag{13}$$

at any point of the reference ray Ω. Eq. (13) is identical to (9).

2.3 Propagator matrix in ray-centred coordinates

Let us now consider an orthonomic system of rays, in which each ray is specified by two ray parameters γ_1, γ_2. The ray parameters γ_1, γ_2 may be chosen in different ways; they may represent the take-off angles at a point source, curvilinear Gaussian coordinates of initial points of rays at a specified initial surface, etc. Along a selected reference ray, we introduce the 2×2 matrices $\mathbf{Q}^{(q)}$ and $\mathbf{P}^{(q)}$, with elements $Q_{IJ}^{(q)} = \partial q_I/\partial\gamma_J$, $P_{IJ}^{(q)} = \partial p_I^{(q)}/\partial\gamma_J$, where $p_I^{(q)} = \partial T/\partial q_I$ are slowness vector components in ray-centred coordinates. The expressions $Q_{IJ}^{(q)}$ and $P_{IJ}^{(q)}$ show how q_I and $p_I^{(q)}$ vary when parameters γ_1, γ_2 change (i.e. from one paraxial ray to another). The 2×2 matrices $\mathbf{Q}^{(q)}$ and $\mathbf{P}^{(q)}$ can be computed by solving a system of linear ordinary differential equations of the first order along the reference ray, called the dynamic ray tracing system, or also the paraxial ray tracing system (Klimeš 1994).

Let us consider two arbitrary points S and R at the reference ray. Solving twice the dynamic ray tracing along the reference ray, with initial condition given at S, once for normalized plane wavefront initial conditions $\mathbf{Q}^{(q)}(S) = \mathbf{I}$ and $\mathbf{P}^{(q)}(S) = \mathbf{0}$, and once for normalized point source initial conditions $\mathbf{Q}^{(q)}(S) = \mathbf{0}$, $\mathbf{P}^{(q)}(S) = \mathbf{I}$, we obtain the 4×4 propagator matrix $\mathbf{\Pi}^{(q)}(R, S)$ in ray-centred coordinates from S to R,

$$\mathbf{\Pi}^{(q)}(R, S) = \begin{pmatrix} \mathbf{Q}_1^{(q)}(R, S) & \mathbf{Q}_2^{(q)}(R, S) \\ \mathbf{P}_1^{(q)}(R, S) & \mathbf{P}_2^{(q)}(R, S) \end{pmatrix} , \tag{14}$$

subject to initial conditions at the point S:

$$\mathbf{\Pi}^{(q)}(S, S) = \mathbf{I} , \tag{15}$$

where $\mathbf{I}$ is the 4×4 identity matrix. For more details on dynamic ray tracing and on the ray propagator matrix $\mathbf{\Pi}^{(q)}(R, S)$ in ray-centred coordinates see, for example, Klimeš (1994) and Červený (2001).

The ray propagator matrix finds many applications in paraxial ray theory. Among others, it may be used to describe a complete four-parametric system of paraxial rays in the vicinity of the reference ray between points S and R:

$$\begin{pmatrix} \mathbf{q}^R \\ \mathbf{p}^{(q)R} \end{pmatrix} = \mathbf{\Pi}^{(q)}(R, S) \begin{pmatrix} \mathbf{q}^S \\ \mathbf{p}^{(q)S} \end{pmatrix} . \tag{16}$$

The 2×1 column matrices (2-D vectors) $\mathbf{q}^R$, $\mathbf{q}^S$, $\mathbf{p}^{(q)R}$ and $\mathbf{p}^{(q)S}$ are given by relations

$$\mathbf{q}^R = \left(q_1^R, q_2^R\right)^T , \qquad \mathbf{q}^S = \left(q_1^S, q_2^S\right)^T ,$$
$$\mathbf{p}^{(q)R} = \left(p_1^{(q)R}, p_2^{(q)R}\right)^T , \qquad \mathbf{p}^{(q)S} = \left(p_1^{(q)S}, p_2^{(q)S}\right)^T . \tag{17}$$

The symbols q_1^R, q_2^R, q_1^S and q_2^S denote the ray-centred coordinates of the paraxial points R' and S', situated in the planes tangent to the wavefronts at R and S, respectively. In these planes $\mathbf{q}$ form 2-D Cartesian coordinate systems. The symbols $p_1^{(q)R}$, $p_2^{(q)R}$, $p_1^{(q)S}$ and $p_2^{(q)S}$ are the corresponding ray-centred components of the slowness vectors at paraxial points R' and S'. We emphasize that the slowness vectors $\mathbf{p}^{(q)R}$ and $\mathbf{p}^{(q)S}$ correspond to the paraxial points R' and S', not to the reference ray Ω, $\mathbf{p}^{(q)R} = \mathbf{p}^{(q)}(R')$, $\mathbf{p}^{(q)S} = \mathbf{p}^{(q)}(S')$. Along the reference ray, the 2×1 column matrices $\mathbf{q}$ and $\mathbf{p}^{(q)}$ vanish.

Eq. (16) may be used both for initial-value ray tracing and for two-point ray tracing of paraxial rays.

In the 'initial-value ray tracing' for paraxial rays, the quantities $\mathbf{q}^S$ and $\mathbf{p}^{(q)S}$ are given and the quantities $\mathbf{q}^R$ and $\mathbf{p}^{(q)R}$ are computed. In other words, the position of the point S'(expressed in ray-centred coordinates q_I^S) and the relevant ray-centred components of the slowness vector at $S'(p_I^{(q)S})$ are given, and the position of the point R'(expressed in ray-centred coordinates q_I^R) and the relevant ray-centred components of the slowness vector at R' $(p_I^{(q)R})$ are computed. Consequently, the position of the point R' is not known in advance, its coordinates $\mathbf{q}^R$ are computed using (16).

Eq. (16) can be also used for 'two-point ray tracing' of paraxial rays, from S' to R'. In this case, the ray-centred coordinates $\mathbf{q}^S$ of point S' and $\mathbf{q}^R$ of point R' are given, and slowness vectors $\mathbf{p}^{(q)S}$ and $\mathbf{p}^{(q)R}$ are not known, but sought. They are functions of both $\mathbf{q}^R$ and $\mathbf{q}^S$:

$$\mathbf{p}^{(q)S} = \mathbf{p}^{(q)S}\left(\mathbf{q}^R, \mathbf{q}^S\right) , \quad \mathbf{p}^{(q)R} = \mathbf{p}^{(q)R}\left(\mathbf{q}^R, \mathbf{q}^S\right) . \tag{18}$$

The relevant two-point paraxial traveltime $T(R', S')$ from S' to R' is also a function of both $\mathbf{q}^R$ and $\mathbf{q}^S$:

$$T(R', S') = T\left(\mathbf{q}^R, \mathbf{q}^S\right) . \tag{19}$$

The relations between the two-point paraxial traveltime (19) and ray-centred components of the slowness vectors (18) are as follows:

$$\frac{\partial T\left(\mathbf{q}^R, \mathbf{q}^S\right)}{\partial q_I^R} = p_I^{(q)R} , \quad \frac{\partial T\left(\mathbf{q}^R, \mathbf{q}^S\right)}{\partial q_I^S} = -p_I^{(q)S} . \tag{20}$$

The first equation in (20) applies to the plane tangent to the wavefront at R, and the second equation to the plane tangent to the wavefront at S. Note the sign minus in the second equation of (20). Eqs (20) for the relations between the two-point traveltime $T(\mathbf{q}^R, \mathbf{q}^S)$ and the components of the relevant slowness vectors $p_I^{(q)R}$ and $p_I^{(q)S}$ have been well known in optical literature for a long time. In Cartesian coordinates, they were discussed in detail already by Hamilton in his studies of characteristic functions (Hamilton 1837). His discussion, however, does not include ray propagator matrices, which were not known in that time. Consequently, he was not able to derive equations for the two-point paraxial traveltime (i.e. the characteristic function in the vicinity of some known reference ray), as we do it in this paper. See also Arnaud (1971, eqs 1a, 1b) and Klimeš (2009, eqs 32 and 33).

3 TWO-POINT PARAXIAL TRAVELTIME IN RAY-CENTRED COORDINATES

In this section, we derive important auxiliary formulae, which are used in the next section for the derivation of two-point paraxial traveltime formula between points arbitrarily chosen in paraxial vicinities of points S and R. We use eqs (16) and (20) to determine

the two-point paraxial traveltime $T(R', S')$ between points S' and R' situated in planes tangent to the wavefronts at S and R on Ω, respectively, and specified by ray-centred coordinates $\mathbf{q}^S$ and $\mathbf{q}^R$. We assume that the points S' and R' are situated in paraxial vicinities of S and R, respectively.

We assume that $\mathbf{q}^S$ and $\mathbf{q}^R$ are given and we use (16) to determine $\mathbf{p}^{(q)S}$ and $\mathbf{p}^{(q)R}$. For this purpose, we rewrite (16) into the form

$$\begin{aligned} \mathbf{q}^R &= \mathbf{Q}_1^{(q)}\mathbf{q}^S + \mathbf{Q}_2^{(q)}\mathbf{p}^{(q)S} , \\ \mathbf{p}^{(q)R} &= \mathbf{P}_1^{(q)}\mathbf{q}^S + \mathbf{P}_2^{(q)}\mathbf{p}^{(q)S} . \end{aligned} \tag{21}$$

Eqs (21) then yield

$$\begin{aligned} \mathbf{p}^{(q)S} &= -\mathbf{Q}_2^{(q)-1}\mathbf{Q}_1^{(q)}\mathbf{q}^S + \mathbf{Q}_2^{(q)-1}\mathbf{q}^R , \\ \mathbf{p}^{(q)R} &= -\mathbf{Q}_2^{(q)-T}\mathbf{q}^S + \mathbf{P}_2^{(q)}\mathbf{Q}_2^{(q)-1}\mathbf{q}^R . \end{aligned} \tag{22}$$

We assume that $\mathbf{Q}_2^{(q)}$ is invertible at R, that is, that there is not caustics at R. In the derivation of (22), we used the symplectic properties of the propagator matrix (14), namely $\mathbf{P}_1^{(q)} - \mathbf{P}_2^{(q)}\mathbf{Q}_2^{(q)-1}\mathbf{Q}_1^{(q)} = -\mathbf{Q}_2^{(q)-T}$, see Červený (2001, eq. 4.3.16).

From (22) with (20), we can also simply determine the second partial derivatives of the two-point paraxial traveltime $T(\mathbf{q}^R, \mathbf{q}^S)$ with respect to ray-centred coordinates q_I^R and q_I^S. We obtain

$$\begin{aligned} \frac{\partial^2 T(\mathbf{q}^R, \mathbf{q}^S)}{\partial q_I^S \partial q_J^S} &= \frac{\partial}{\partial q_J^S}\left(-p_I^{(q)S}\right) = \left(\mathbf{Q}_2^{(q)-1}\mathbf{Q}_1^{(q)}\right)_{IJ} , \\ \frac{\partial^2 T(\mathbf{q}^R, \mathbf{q}^S)}{\partial q_I^R \partial q_J^R} &= \frac{\partial}{\partial q_J^R}\left(p_I^{(q)R}\right) = \left(\mathbf{P}_2^{(q)}\mathbf{Q}_2^{(q)-1}\right)_{IJ} , \\ \frac{\partial^2 T(\mathbf{q}^R, \mathbf{q}^S)}{\partial q_I^S \partial q_J^R} &= \frac{\partial}{\partial q_J^R}\left(-p_I^{(q)S}\right) = \left(-\mathbf{Q}_2^{(q)-1}\right)_{IJ} , \\ \frac{\partial^2 T(\mathbf{q}^R, \mathbf{q}^S)}{\partial q_I^R \partial q_J^S} &= \frac{\partial}{\partial q_J^S}\left(p_I^{(q)R}\right) = \left(-\mathbf{Q}_2^{(q)-T}\right)_{IJ} . \end{aligned} \tag{23}$$

The expressions for the second derivatives of $T(\mathbf{q}^R, \mathbf{q}^S)$ do not depend on ray-centred coordinates $\mathbf{q}^R$ and $\mathbf{q}^S$. Actually, they can be expressed in terms of the 2×2 submatrices of the ray propagator matrix (14), computed along the reference ray Ω.

As we know expressions for the first and second partial derivatives of $T(\mathbf{q}^R, \mathbf{q}^S)$, we can write the Taylor expansion for $T(\mathbf{q}^R, \mathbf{q}^S)$ in terms of q_I^R and q_I^S $(I, J = 1, 2)$, up to the quadratic terms:

$$\begin{aligned} T(\mathbf{q}^R, \mathbf{q}^S) = T(R, S) &+ q_I^R \left(\frac{\partial T(\mathbf{q}^R, \mathbf{q}^S)}{\partial q_I^R}\right)_\Omega + q_I^S \left(\frac{\partial T(\mathbf{q}^R, \mathbf{q}^S)}{\partial q_I^S}\right)_\Omega \\ &+ \frac{1}{2} q_I^R \left(\frac{\partial^2 T(\mathbf{q}^R, \mathbf{q}^S)}{\partial q_I^R \partial q_J^R}\right)_\Omega q_J^R + \frac{1}{2} q_I^S \left(\frac{\partial^2 T(\mathbf{q}^R, \mathbf{q}^S)}{\partial q_I^S \partial q_J^S}\right)_\Omega q_J^S \\ &+ \frac{1}{2} q_I^S \left(\frac{\partial^2 T(\mathbf{q}^R, \mathbf{q}^S)}{\partial q_I^S \partial q_J^R}\right)_\Omega q_J^R + \frac{1}{2} q_I^R \left(\frac{\partial^2 T(\mathbf{q}^R, \mathbf{q}^S)}{\partial q_I^R \partial q_J^S}\right)_\Omega q_J^S . \end{aligned} \tag{24}$$

All the coefficients in the Taylor series (24) are taken for $\mathbf{q}^R = \mathbf{q}^S = \mathbf{0}$, that is, on the reference ray Ω. This fact is emphasized by the parentheses with the subscript Ω.

We now take into account that

$$q_I^S \frac{\partial^2 T(\mathbf{q}^R, \mathbf{q}^S)}{\partial q_I^S \partial q_J^R} q_J^R = q_I^R \frac{\partial^2 T(\mathbf{q}^R, \mathbf{q}^S)}{\partial q_I^R \partial q_J^S} q_J^S , \tag{25}$$

and that the linear terms in (24) vanish, as $\mathbf{p}^{(q)R} = \mathbf{p}^{(q)S} = \mathbf{0}$ on the reference ray Ω. When we insert (23) into (24) and use the notation (19), we finally obtain the following:

$$\begin{aligned} T(R', S') = T(R, S) &+ \tfrac{1}{2} q_I^R \left(\mathbf{P}_2^{(q)}\mathbf{Q}_2^{(q)-1}\right)_{IJ} q_J^R \\ &+ \tfrac{1}{2} q_I^S \left(\mathbf{Q}_2^{(q)-1}\mathbf{Q}_1^{(q)}\right)_{IJ} q_J^S - q_I^S \left(\mathbf{Q}_2^{(q)-1}\right)_{IJ} q_J^R . \end{aligned} \tag{26}$$

This can be rewritten in a matrix form

$$\begin{aligned} T(R', S') = T(R, S) &+ \tfrac{1}{2} \left(\mathbf{q}^R\right)^T \mathbf{P}_2^{(q)}\mathbf{Q}_2^{(q)-1}\mathbf{q}^R \\ &+ \tfrac{1}{2} \left(\mathbf{q}^S\right)^T \mathbf{Q}_2^{(q)-1}\mathbf{Q}_1^{(q)}\mathbf{q}^S - \left(\mathbf{q}^S\right)^T \mathbf{Q}_2^{(q)-1}\mathbf{q}^R . \end{aligned} \tag{27}$$

A similar approach as presented here to derive $T(R', S')$ for inhomogeneous anisotropic media was used by Arnaud (1971) and by Červený (2001) for inhomogeneous isotropic media. Note that there is no linear term in $\mathbf{q}$ in (27) because of the definition of ray-centred coordinates.

Let us emphasize again that eqs (26) and (27) are applicable only if the points R' and S' are situated in planes tangent to the wavefronts at R and S, respectively. The situation that R' and S' are situated arbitrarily in the vicinity of R and S will be treated in Section 4.

By squaring (27) and discarding terms of higher order than two, we can easily derive an approximate relation for $T^2(R', S')$:

$$\begin{aligned} T^2(R', S') = T^2(R, S) &+ T(R, S)\big[(\mathbf{q}^R)^T \mathbf{P}_2^{(q)}\mathbf{Q}_2^{(q)-1}\mathbf{q}^R \\ &+ (\mathbf{q}^S)^T \mathbf{Q}_2^{(q)-1}\mathbf{Q}_1^{(q)}\mathbf{q}^S - 2(\mathbf{q}^S)^T \mathbf{Q}_2^{(q)-1}\mathbf{q}^R\big] . \end{aligned} \tag{28}$$

Note that the 2×2 submatrix $\mathbf{P}_1^{(q)}$ is not needed in the computation of $T(R', S')$ and $T^2(R', S')$ because of the symplectic properties of ray propagator matrix (14).

4 TWO-POINT PARAXIAL TRAVELTIME IN CARTESIAN COORDINATES

We now use the ray propagator matrix (14) in ray-centred coordinates to derive the equation for the two-point paraxial traveltime $T(R', S')$ and for the corresponding paraxial slowness vectors in Cartesian coordinates. In this case the points R' and S' can be situated arbitrarily in the 3-D paraxial vicinity of R and S, respectively. It is not required that R' and S' are situated in a plane tangential to the wavefront at R and S, as in ray-centred coordinates in (26). In the derivation, we shall need to transform the second-order two-point traveltime derivatives from ray-centred to Cartesian coordinates.

First, let us write the Taylor expansion for $T(R', S')$ in terms of δx_i^R and δx_i^S $(i = 1, 2, 3)$ up to the quadratic terms, where

$$\delta x_i^R = x_i(R') - x_i(R) , \qquad \delta x_i^S = x_i(S') - x_i(S) . \tag{29}$$

Similarly as in (24), we can write

$$\begin{aligned} T(R', S') = T(R, S) &+ \delta x_i^R \left(\frac{\partial T(R', S')}{\partial x_i^R}\right)_\Omega + \delta x_i^S \left(\frac{\partial T(R', S')}{\partial x_i^S}\right)_\Omega \\ &+ \frac{1}{2} \delta x_i^R \left(\frac{\partial^2 T(R', S')}{\partial x_i^R \partial x_j^R}\right)_\Omega \delta x_j^R + \frac{1}{2} \delta x_i^S \left(\frac{\partial^2 T(R', S')}{\partial x_i^S \partial x_j^S}\right)_\Omega \delta x_j^S \\ &+ \delta x_i^S \left(\frac{\partial^2 T(R', S')}{\partial x_i^S \partial x_j^R}\right)_\Omega \delta x_j^R . \end{aligned} \tag{30}$$

Here the two-point traveltime $T(R', S')$ is now expressed in terms of Cartesian coordinates, $T(R', S') = T(\delta x_i^R, \delta x_i^S)$. Taking into account (20), we get for coefficients of linear terms:

$$\left(\partial T(R', S')/\partial x_i^R\right)_\Omega = p_i(R) , \quad \left(\partial T(R', S')/\partial x_i^S\right)_\Omega = -p_i(S) , \tag{31}$$

where $p_i(R)$ and $p_i(S)$ are components of slowness vectors on the reference ray Ω, at R and S, respectively.

It remains to determine the coefficients of the quadratic terms. They can be determined by transforming the second-order two-point traveltime derivatives in ray-centred coordinates to second-order two-point traveltime derivatives in Cartesian coordinates. The corresponding transformation relations were derived in Červený & Klimeš (2010, eqs 23 and 36), and at the point R read

$$\frac{\partial^2 T}{\partial x_i^R \partial x_j^R} = \frac{\partial q_M^R}{\partial x_i^R} \frac{\partial^2 T}{\partial q_M^R \partial q_N^R} \frac{\partial q_N^R}{\partial x_j^R} + \frac{\partial^2 q_3}{\partial x_i^R \partial x_j^R} . \tag{32}$$

It is further shown there that the term

$$\frac{\partial^2 q_3}{\partial x_i^R \partial x_j^R} = \Phi_{ij}(R) \tag{33}$$

can be expressed as

$$\Phi_{ij}(R) = (p_i \eta_j + p_j \eta_i - p_i p_j \mathcal{U}_k \eta_k)_R . \tag{34}$$

Eq. (32) can be then rewritten as

$$\frac{\partial^2 T}{\partial x_i^R \partial x_j^R} = f_{Mi}^R \frac{\partial^2 T}{\partial q_M^R \partial q_N^R} f_{Nj}^R + \Phi_{ij}(R) , \tag{35}$$

where we took into account relations (11). The Cartesian components of vectors $\mathbf{p}, \boldsymbol{\mathcal{U}}$ and $\boldsymbol{\eta}$ at R in (34) are known from ray tracing so that $\Phi_{ij}(R)$ may be easily computed at any point of the reference ray Ω. Note that $\Phi_{ij}(R) = \Phi_{ji}(R)$. The transformation relation at the point S is quite analogous:

$$\frac{\partial^2 T}{\partial x_i^S \partial x_j^S} = f_{Mi}^S \frac{\partial^2 T}{\partial q_M^S \partial q_N^S} f_{Nj}^S - \Phi_{ij}(S) , \tag{36}$$

where

$$\Phi_{ij}(S) = (p_i \eta_j + p_j \eta_i - p_i p_j \mathcal{U}_k \eta_k)_S , \tag{37}$$

and where we took into account (20) when specifying the sign at $\Phi_{ij}(S)$.

The transformation relations for the mixed second derivatives $\partial^2 T / \partial x_i^R \partial x_j^S$ are simpler. It is obvious that the term $\partial^2 q_3^S / \partial x_i^R \partial x_j^S$ is zero because the coordinate q_3^S of the point S does not depend on the coordinates x_i^R of the point R. Consequently, at the point R, we obtain

$$\frac{\partial^2 T}{\partial x_i^R \partial x_j^S} = f_{Mi}^R \frac{\partial^2 T}{\partial q_M^R \partial q_N^S} f_{Nj}^S . \tag{38}$$

The same holds for q_3^R differentiated with respect to x_i^S. Consequently, we obtain

$$\frac{\partial^2 T}{\partial x_i^S \partial x_j^R} = f_{Mi}^S \frac{\partial^2 T}{\partial q_M^S \partial q_N^R} f_{Nj}^R . \tag{39}$$

We can now insert (31), (35), (36), (38) and (39) into (30) and replace the second derivatives of the two-point traveltime field by the submatrices of the ray propagator matrix in ray-centred coordinates using (23). This yields

$$\begin{aligned} T(R', S') = {} & T(R, S) + \delta x_i^R p_i(R) - \delta x_i^S p_i(S) \\ & + \tfrac{1}{2} \delta x_i^R \big[f_{Mi}^R \, (\mathbf{P}_2^{(q)} \mathbf{Q}_2^{(q)-1})_{MN} \, f_{Nj}^R + \Phi_{ij}(R) \big] \delta x_j^R \\ & + \tfrac{1}{2} \delta x_i^S \big[f_{Mi}^S \, (\mathbf{Q}_2^{(q)-1} \mathbf{Q}_1^{(q)})_{MN} \, f_{Nj}^S - \Phi_{ij}(S) \big] \delta x_j^S \\ & - \delta x_i^S \big[f_{Mi}^S \, (\mathbf{Q}_2^{(q)-1})_{MN} \, f_{Nj}^R \big] \delta x_j^R . \end{aligned} \tag{40}$$

Let us emphasize again that eq. (40) gives the expression for the two-point paraxial traveltime $T(R', S')$ in Cartesian coordinates (29), but uses the 2×2 submatrices $\mathbf{Q}_1^{(q)}$, $\mathbf{Q}_2^{(q)}$ and $\mathbf{P}_2^{(q)}$ of the 4×4 ray propagator matrix (14) in ray-centred coordinates. The knowledge of the 6×6 ray propagator matrix in Cartesian coordinates is not required here. See Section 5 for an alternative derivation of $T(R', S')$ in Cartesian coordinates using the 6×6 ray propagator matrix in Cartesian coordinates.

It may be useful to introduce 3×3 matrices of second derivatives of traveltime $\mathbf{F}^{RR}$, $\mathbf{F}^{SS}$ and $\mathbf{F}^{SR}$, with elements

$$\begin{aligned} F_{ij}^{RR} &= f_{Mi}^R \big(\mathbf{P}_2^{(q)} \mathbf{Q}_2^{(q)-1} \big)_{MN} \, f_{Nj}^R , \\ F_{ij}^{SS} &= f_{Mi}^S \big(\mathbf{Q}_2^{(q)-1} \mathbf{Q}_1^{(q)} \big)_{MN} \, f_{Nj}^S , \\ F_{ij}^{SR} &= f_{Mi}^S \big(\mathbf{Q}_2^{(q)-1} \big)_{MN} \, f_{Nj}^R . \end{aligned} \tag{41}$$

Then the expression (40) for the two-point paraxial traveltime $T(R', S')$ can be expressed in a simple final form

$$\begin{aligned} T(R', S') = {} & T(R, S) + \delta x_i^R p_i(R) - \delta x_i^S p_i(S) \\ & + \tfrac{1}{2} \delta x_i^R \big(F_{ij}^{RR} + \Phi_{ij}(R) \big) \delta x_j^R + \tfrac{1}{2} \delta x_i^S \big(F_{ij}^{SS} - \Phi_{ij}(S) \big) \delta x_j^S \\ & - \delta x_i^S F_{ij}^{SR} \delta x_j^R . \end{aligned} \tag{42}$$

Here $p_i(R)$, $p_i(S)$, $\Phi_{ij}(R)$ and $\Phi_{ij}(S)$ are known from ray tracing, $\mathbf{Q}_1^{(q)}$, $\mathbf{Q}_2^{(q)}$ and $\mathbf{P}_2^{(q)}$ from dynamic ray tracing along Ω. The vectors $\mathbf{f}_M^R$ and $\mathbf{f}_M^S$ can be computed as described in Section 2.2, eqs (6), (7) and (12).

Similarly as in (28), we can easily compute the relation for $T^2(R', S')$ from (42):

$$\begin{aligned} T^2(R', S') = {} & \big[T(R, S) + \delta x_i^R p_i(R) - \delta x_i^S p_i(S) \big]^2 \\ & + T(R, S) \big[\delta x_i^R \big(F_{ij}^{RR} + \Phi_{ij}(R) \big) \delta x_j^R + \delta x_i^S \big(F_{ij}^{SS} - \Phi_{ij}(S) \big) \delta x_j^S \\ & - 2 \delta x_i^S F_{ij}^{SR} \delta x_j^R \big] . \end{aligned} \tag{43}$$

Using eq. (42) for a two-point paraxial traveltime $T(R', S')$, and remembering that, because of (20), derivatives with respect to x_i^S must be taken with opposite signs, we can simply derive expressions for the paraxial slowness vectors at S' and R'. We obtain

$$\begin{aligned} p_i(R') &= \partial T(R', S') / \partial x_i^R \\ &= p_i(R) + \big[F_{ij}^{RR} + \Phi_{ij}(R) \big] \delta x_j^R - F_{ji}^{SR} \delta x_j^S , \\ p_i(S') &= -\partial T(R', S') / \partial x_i^S \\ &= p_i(S) - \big[F_{ij}^{SS} - \Phi_{ij}(S) \big] \delta x_j^S + F_{ij}^{SR} \delta x_j^R . \end{aligned} \tag{44}$$

As we can see from (40), the two-point paraxial traveltime $T(R', S')$ in Cartesian coordinates is expressed in terms of covariant basis vectors $\mathbf{f}_1^R$, $\mathbf{f}_2^R$, $\mathbf{f}_1^S$ and $\mathbf{f}_2^S$, perpendicular to the reference ray Ω at R and S.

A brief note to the eq. (42). As we can see from it, the elements F_{ij}^{SR} of the 3×3 matrix $\mathbf{F}^{SR}$ represent the mixed second-order partial derivatives of $T(R', S')$ with respect to Cartesian coordinates δx_i^S and δx_j^R. We speak of mixed second-order derivatives as they are related to both points S and R. The mixed second-order partial derivatives F_{ij}^{SR} can be used to determine the 2×2 matrix of geometrical spreading $\mathbf{Q}_2^{(q)}$ [see the last equation in (41)] needed in the computation of ray amplitudes along the reference ray. Consequently, the geometrical spreading can be determined from the actual paraxial traveltime measurements at S and R; the dynamic ray tracing along the reference ray is not necessary.

5 ALTERNATIVE FORM OF TWO-POINT PARAXIAL TRAVELTIME FORMULA IN CARTESIAN COORDINATES

In this section, the dynamic ray tracing and 6×6 propagator matrix in Cartesian coordinates are used for the direct derivation of the two-point paraxial traveltime formula in Cartesian coordinates. No transformations are, therefore, required.

Let us denote the 6×6 ray propagator matrix in Cartesian coordinates between points S and R on the reference ray by $\mathbf{\Pi}^{(x)}(R, S)$. It corresponds to Hamiltonian function (1), and can be expressed as

$$\mathbf{\Pi}^{(x)}(R, S) = \begin{pmatrix} \mathbf{Q}_1^{(x)}(R, S) & \mathbf{Q}_2^{(x)}(R, S) \\ \mathbf{P}_1^{(x)}(R, S) & \mathbf{P}_2^{(x)}(R, S) \end{pmatrix} . \tag{45}$$

Here the submatrices $\mathbf{Q}_1^{(x)}$, $\mathbf{Q}_2^{(x)}$, $\mathbf{P}_1^{(x)}$ and $\mathbf{P}_2^{(x)}$ are of the size 3×3.

To emphasize the difference between the 6×6 ray propagator matrix $\mathbf{\Pi}^{(x)}(R, S)$ in Cartesian coordinates given in (45) and the 4×4 ray propagator matrix $\mathbf{\Pi}^{(q)}(R, S)$ in ray-centred coordinates given in (14), we use the superscripts (x) and (q). The same superscripts are used in the 3×3 submatrices $\mathbf{Q}_1^{(x)}$, $\mathbf{Q}_2^{(x)}$, $\mathbf{P}_1^{(x)}$ and $\mathbf{P}_2^{(x)}$ in Cartesian coordinates in (45) and in the 2×2 submatrices $\mathbf{Q}_1^{(q)}$, $\mathbf{Q}_2^{(q)}$, $\mathbf{P}_1^{(q)}$ and $\mathbf{P}_2^{(q)}$ in ray-centred coordinates in (14).

Let us now evaluate coefficients of the Taylor expansion (30) for $T(R', S')$ using the matrix $\mathbf{\Pi}^{(x)}(R, S)$. Coefficients of linear terms follow again from (31). For coefficients of quadratic terms, we can use results derived by Klimeš (2009, equations 34– 36), and obtain

$$\begin{aligned}
\left(\frac{\partial^2 T(R', S')}{\partial x_i^R \partial x_j^R}\right)_\Omega &= \left[\mathbf{P}_2^{(x)}(R, S)\mathbf{Q}_2^{(x)-1}(R, S)\right]_{ij} \\
&\quad - T^{-1}(R, S) p_i(R) p_j(R) , \\
\left(\frac{\partial^2 T(R', S')}{\partial x_i^S \partial x_j^S}\right)_\Omega &= \left[\mathbf{Q}_2^{(x)-1}(R, S)\mathbf{Q}_1^{(x)}(R, S)\right]_{ij} \\
&\quad - T^{-1}(R, S) p_i(S) p_j(S) , \\
\left(\frac{\partial^2 T(R', S')}{\partial x_i^S \partial x_j^R}\right)_\Omega &= \left[- \mathbf{Q}_2^{(x)-1}(R, S)\right]_{ij} + T^{-1}(R, S) p_i(S) p_j(R) .
\end{aligned} \tag{46}$$

Here $p_i(S)$ and $p_i(R)$ are Cartesian components of the slowness vector on the reference ray, at points S and R. The terms with $T^{-1}(R, S)$ in (46) have an origin in the non-eikonal solutions of dynamic ray tracing equations included in the 6×6 ray propagator matrix (45). The expressions (46) become singular for $R \to S$ because $\mathbf{Q}_2^{(x)}(R, S) \to 0$ and $T(R, S) \to 0$. Inserting (31) and (46) to (30), we get the final equation for $T(R', S')$ in Cartesian coordinates:

$$\begin{aligned}
T(R', S') &= T(R, S) + \delta x_i^R p_i(R) - \delta x_i^S p_i(S) \\
&- \frac{1}{2} T^{-1}(R, S)\left[\delta x_i^R p_i(R) - \delta x_i^S p_i(S)\right]^2 + \frac{1}{2}\delta x_i^R \left(\mathbf{P}_2^{(x)}\mathbf{Q}_2^{(x)-1}\right)_{ij}\delta x_j^R \\
&+ \frac{1}{2}\delta x_i^S \left(\mathbf{Q}_2^{(x)-1}\mathbf{Q}_1^{(x)}\right)_{ij}\delta x_j^S - \delta x_i^S \left(\mathbf{Q}_2^{(x)-1}\right)_{ij}\delta x_j^R .
\end{aligned} \tag{47}$$

This is an alternative form of eq. (40). Similarly as the expressions in (46), the expression (47) is singular for $R \to S$. In contrast to (26), the linear terms in (47) are, in general, non-vanishing, similarly as in (42). Eq. (47) does not require knowledge of vectors $\mathbf{f}_M$ at S and R. On the other hand, evaluation of 3×3 matrices $\mathbf{Q}_1^{(x)}$, $\mathbf{Q}_2^{(x)}$ and $\mathbf{P}_2^{(x)}$ requires solution of 36 dynamic ray tracing equations along the reference ray Ω. In case of 2×2 matrices $\mathbf{Q}_1^{(q)}$, $\mathbf{Q}_2^{(q)}$ and $\mathbf{P}_2^{(q)}$ used in (40), it is only 16 dynamic ray tracing equations, plus three additional equations covering the propagation of basis vectors along the ray, eq. (6).

Neglecting the terms of the order higher than two in δx_i^S, δx_j^R, we get from (47) the expression for the two-point paraxial traveltime squared:

$$\begin{aligned}
T^2(R', S') &= T^2(R, S) + 2T(R, S)\left[\delta x_i^R p_i(R) - \delta x_i^S p_i(S)\right] \\
&+ T(R, S)\left[\delta x_i^R \left(\mathbf{P}_2^{(x)}\mathbf{Q}_2^{(x)-1}\right)_{ij}\delta x_j^R + \delta x_i^S \left(\mathbf{Q}_2^{(x)-1}\mathbf{Q}_1^{(x)}\right)_{ij}\delta x_j^S \right. \\
&\left. - 2\delta x_i^S \left(\mathbf{Q}_2^{(x)-1}\right)_{ij}\delta x_j^R\right] .
\end{aligned} \tag{48}$$

Eq. (48) represents an alternative form of eq. (43). We can see that it has simpler form than (47), and it is also simpler than (43). In contrast to expressions (42), (43) and (47), coefficients of quadratic terms in (48) do not depend explicitly on slowness vectors $\mathbf{p}(S)$ and $\mathbf{p}(R)$. Coefficients of quadratic terms in (48) depend solely on submatrices of the ray propagator matrix $\mathbf{\Pi}^{(x)}(R, S)$ multiplied by $T(R, S)$.

We observe that eq. (48) is analogous to eq. (28) in the way the coefficients of quadratic terms depend on the relevant submatrices of the ray propagator matrix ($\mathbf{\Pi}^{(x)}(R, S)$ or $\mathbf{\Pi}^{(q)}(R, S)$). While eq. (28) allows calculation of the two-point traveltime squared $T^2(R', S')$ only between points S' and R' situated in planes tangent to wavefronts at points S and R, eq. (48) allows calculation of $T^2(R', S')$ between points S' and R' arbitrarily chosen in vicinities of S and R, respectively.

From eq. (47), we can obtain expressions for the paraxial slowness vectors $\mathbf{p}(S')$ and $\mathbf{p}(R')$:

$$\begin{aligned}
p_i(R') &= p_i(R) - T^{-1}(R, S) p_i(R)\left[p_j(R)\delta x_j^R - p_j(S)\delta x_j^S\right] \\
&\quad + \left(\mathbf{P}_2^{(x)}\mathbf{Q}_2^{(x)-1}\right)_{ij}\delta x_j^R - \left(\mathbf{Q}_2^{(x)-1}\right)_{ji}\delta x_j^S , \\
p_i(S') &= p_i(S) - T^{-1}(R, S) p_i(S)\left[p_j(R)\delta x_j^R - p_j(S)\delta x_j^S\right] \\
&\quad - \left(\mathbf{Q}_2^{(x)-1}\mathbf{Q}_1^{(x)}\right)_{ij}\delta x_j^S + \left(\mathbf{Q}_2^{(x)-1}\right)_{ij}\delta x_j^R .
\end{aligned} \tag{49}$$

By differentiating eq. (48) it is straightforward to obtain corresponding equations for paraxial slowness vectors associated with the two-point traveltime squared.

6 SPECIAL CASES

Eqs (42) and (47) for the two-point paraxial traveltime $T(R', S')$ derived using the ray propagator matrices in ray-centred and Cartesian coordinates, respectively, and related eqs (44) and (49) for the paraxial slowness vectors $\mathbf{p}(R')$ and $\mathbf{p}(S')$, are very general. They simplify in some special cases. Here we consider several such cases.

6.1 Homogeneous anisotropic media

For homogeneous anisotropic media, vector $\boldsymbol{\eta} = \mathrm{d}\mathbf{p}(\tau)/\mathrm{d}\tau = \mathbf{0}$, as $\mathbf{p}(\tau)$ remains constant along the ray. Consequently, the terms $\Phi_{ij}(R)$ and $\Phi_{ij}(S)$ in (42) and (44) become also zero, see (34) and (37). Further, for the 2×2 submatrices $\mathbf{Q}_1^{(q)}(R, S)$ and $\mathbf{P}_2^{(q)}(R, S)$ of the 4×4 ray propagator matrix (14) we get $\mathbf{Q}_1^{(q)} = \mathbf{I}$ and $\mathbf{P}_2^{(q)} = \mathbf{I}$. The only varying submatrix of (14), which appears in (42) and (44), is $\mathbf{Q}_2^{(q)}(R, S)$. If we take into account that $\mathbf{p}(R) = \mathbf{p}(S)$ and $\mathbf{f}_M^R = \mathbf{f}_M^S$, eqs (42) and (44) yield simplified relations.

$$\begin{aligned}
T(R', S') &= T(R, S) + p_i(S)\left(\delta x_i^R - \delta x_i^S\right) \\
&\quad + \tfrac{1}{2} f_{Mi}^S \left(\mathbf{Q}_2^{(q)-1}\right)_{MN} f_{Nj}^S \left(\delta x_i^R - \delta x_i^S\right)\left(\delta x_j^R - \delta x_j^S\right) ,
\end{aligned} \tag{50}$$

and

$$p_i(R') = p_i(S') = p_i(S) + f_{Mi}^S \left(\mathbf{Q}_2^{(q)-1}\right)_{MN} f_{Nj}^S \left(\delta x_j^R - \delta x_j^S\right) , \tag{51}$$

where $\mathbf{Q}_2^{(q)} = \mathbf{Q}_2^{(q)}(R, S)$ is symmetric. We can see that the slowness vectors at S' and R' are identical since the ray Ω' is, similarly as Ω, a straight line. If $\delta\mathbf{x}^R = \delta\mathbf{x}^S$, we find that $T(R', S') = T(R, S)$ and $\mathbf{p}(R') = \mathbf{p}(S') = \mathbf{p}(R) = \mathbf{p}(S)$; the rays Ω' and Ω are parallel and the traveltime between R' and S' equals the traveltime between R and S.

Eq. (47) reduces for a homogeneous anisotropic medium to

$$\begin{aligned} T(R', S') = {} & T(R, S) + p_i(S)\left(\delta x_i^R - \delta x_i^S\right) \\ & - \tfrac{1}{2} T^{-1}(R, S)\left[p_i(S)\left(\delta x_i^R - \delta x_i^S\right)\right]^2 \\ & + \tfrac{1}{2}\left(\mathbf{Q}_2^{(x)-1}\right)_{ij}\left(\delta x_i^R - \delta x_i^S\right)\left(\delta x_j^R - \delta x_j^S\right) . \end{aligned} \tag{52}$$

Here $\mathbf{Q}_2^{(x)} = \mathbf{Q}_2^{(x)}(R, S)$ is 3×3 upper right submatrix of the 6×6 ray propagator matrix $\mathbf{\Pi}^{(x)}(R, S)$. The symmetric submatrix $\mathbf{Q}_2^{(x)}$ is the only varying submatrix appearing in (52). For submatrices $\mathbf{Q}_1^{(x)}(R, S)$ and $\mathbf{P}_2^{(x)}(R, S)$ we have $\mathbf{Q}_1^{(x)} = \mathbf{P}_2^{(x)} = \mathbf{I}$, and the submatrix $\mathbf{P}_1^{(x)}(R, S)$ is not needed in (52). In (52), we took into account that $\mathbf{p}(R) = \mathbf{p}(S)$. For the slowness vectors at R' and S' we get

$$\begin{aligned} & p_i(R') = p_i(S') = p_i(S) \\ & -T^{-1}(R, S)p_i(S)p_j(S)\left(\delta x_j^R - \delta x_j^S\right) + (\mathbf{Q}_2^{-1})_{ij}\left(\delta x_j^R - \delta x_j^S\right) . \end{aligned} \tag{53}$$

6.2 Coinciding S and S'

For $\delta x_i^S = 0$ (e.g. a point source at S), eq. (42) simplifies considerably:

$$T(R', S) = T(R, S) + \delta x_i^R p_i(R) + \tfrac{1}{2}\delta x_i^R\left(F_{ij}^{RR} + \Phi_{ij}(R)\right)\delta x_j^R . \tag{54}$$

Similarly, the expressions for the paraxial slowness vector components (44) also simplify when $\delta x_i^S = 0$,

$$\begin{aligned} p_i(R') &= p_i(R) + \left[F_{ij}^{RR} + \Phi_{ij}(R)\right]\delta x_j^R , \\ p_i(S') &= p_i(S) + F_{ij}^{SR}\delta x_j^R . \end{aligned} \tag{55}$$

Here $p_i(S')$ denotes the slowness vector taken at S, but corresponding to the paraxial ray Ω' connecting S with R'.

From eq. (47) we get in this case

$$\begin{aligned} T(R', S') = {} & T(R, S) + \delta x_i^R p_i(R) - \tfrac{1}{2} T^{-1}(R, S)\left[p_j(R)\delta x_j^R\right]^2 \\ & + \tfrac{1}{2}\delta x_i^R\left(\mathbf{P}_2^{(x)}\mathbf{Q}_2^{(x)-1}\right)_{ij}\delta x_j^R . \end{aligned} \tag{56}$$

The expressions for the slowness vector components attain the form

$$\begin{aligned} p_i(R') = {} & p_i(R) - T^{-1}(R, S)p_i(R)p_j(R)\delta x_j^R \\ & + \left(\mathbf{P}_2^{(x)}\mathbf{Q}_2^{(x)-1}\right)_{ij}\delta x_j^R , \\ p_i(S') = {} & p_i(S) - T^{-1}(R, S)p_i(S)p_j(R)\delta x_j^R + \left(\mathbf{Q}_2^{(x)-1}\right)_{ij}\delta x_j^R . \end{aligned} \tag{57}$$

Again, $p_i(S')$ denotes the slowness vector taken at S, but corresponding to the paraxial ray Ω' connecting S with R'.

Note that there is no need to compute submatrices $\mathbf{Q}_1$ and $\mathbf{P}_1$ of the ray propagator matrix for a point source situated at S since submatrices $\mathbf{Q}_2$ and $\mathbf{P}_2$ are computed independently. Consequently, the number of differential equations in dynamic ray tracing system is reduced from 16 to 8 in ray-centred coordinates and from 36 to 18 in Cartesian coordinates.

6.3 Coinciding R and R'

For $\delta x_i^R = 0$ (e.g. a point source at R), we obtain from (42)

$$T(R, S') = T(R, S) - \delta x_i^S p_i(S) + \frac{1}{2}\delta x_i^S\left(F_{ij}^{SS} - \Phi_{ij}(S)\right)\delta x_j^S . \tag{58}$$

For paraxial slowness vector components we obtain from (44)

$$\begin{aligned} p_i(R') &= p_i(R) - F_{ji}^{SR}\delta x_j^S , \\ p_i(S') &= p_i(S) - \left[F_{ij}^{SS} - \Phi_{ij}(S)\right]\delta x_j^S . \end{aligned} \tag{59}$$

Here $p_i(R')$ denotes p_i taken at R, but corresponding to the paraxial ray Ω' connecting S' with R.

Eq. (47) yields in this case

$$\begin{aligned} T(R', S') = {} & T(R, S) - \delta x_i^S p_i(S) - \frac{1}{2} T^{-1}(R, S)\left[p_j(S)\delta x_j^S\right]^2 \\ & + \tfrac{1}{2}\delta x_i^S\left(\mathbf{Q}_2^{(x)-1}\mathbf{Q}_1^{(x)}\right)_{ij}\delta x_j^S . \end{aligned} \tag{60}$$

The expressions for the slowness vector components have now the form

$$\begin{aligned} p_i(R') &= p_i(R) + T^{-1}(R, S)p_i(R)p_j(S)\delta x_j^S - \left(\mathbf{Q}_2^{(x)-1}\right)_{ij}\delta x_j^S , \\ p_i(S') &= p_i(S) + T^{-1}(R, S)p_i(S)p_j(S)\delta x_j^S - \left(\mathbf{Q}_2^{(x)-1}\mathbf{Q}_1^{(x)}\right)_{ij}\delta x_j^S . \end{aligned} \tag{61}$$

Again, $p_i(R')$ denotes the slowness vector taken at R, but corresponding to the paraxial ray Ω' connecting S' with R.

Note that computation of submatrices $\mathbf{Q}_1$ and $\mathbf{Q}_2$ of the ray propagator matrix for a point source situated at R requires computation of submatrices $\mathbf{P}_1$ and $\mathbf{P}_2$. Consequently, the number of differential equations in dynamic ray tracing system cannot be reduced in this case.

6.4 Points S' and/or R' in planes tangent to wavefronts at S and/or R

Consider point S' situated in the plane tangent to the wavefront at the point S on the ray Ω. Then we can express δx_i^S in the following form:

$$\delta x_i^S = q_N^S e_{Ni}^S . \tag{62}$$

Here $N = 1, 2$, and q_1^S and q_2^S specify the position of the point S' in the plane. Then

$$\delta x_i^S p_i(S) = 0 , \quad \delta x_i^S \Phi_{ij}(S)\delta x_j^S = 0 , \tag{63}$$

as the slowness vector at the point S is always perpendicular to $\mathbf{e}_1^S$ and $\mathbf{e}_2^S$. Further, using (13), we obtain

$$\delta x_i^S f_{Mi}^S = q_N^S e_{Ni}^S f_{Mi}^S = q_N^S \delta_{NM} = q_M^S . \tag{64}$$

Consequently, (42) yields

$$\begin{aligned} T(R', S') = {} & T(R, S) + \delta x_i^R p_i(R) \\ & + \tfrac{1}{2}\delta x_i^R\left(F_{ij}^{RR} + \Phi_{ij}(R)\right)\delta x_j^R + \tfrac{1}{2} q_M^S\left(\mathbf{Q}_2^{(q)-1}\mathbf{Q}_1^{(q)}\right)_{MN} q_N^S \\ & - q_M^S\left(\mathbf{Q}_2^{(q)-1}\right)_{MN}\delta x_i^R f_{Ni}^R . \end{aligned} \tag{65}$$

Quite analogously, we obtain an expression for $T(R', S')$ if the point R' is situated in the plane tangent to the wavefront at the point R:

$$\begin{aligned} T(R', S') = {} & T(R, S) - \delta x_i^S p_i(S) \\ & + \tfrac{1}{2} q_M^R\left(\mathbf{P}_2^{(q)}\mathbf{Q}_2^{(q)-1}\right)_{MN} q_N^R + \tfrac{1}{2}\delta x_i^S\left(F_{ij}^{SS} - \Phi_{ij}(S)\right)\delta x_i^S \\ & - \delta x_i^S f_{Mi}^S\left(\mathbf{Q}_2^{(q)-1}\right)_{MN} q_N^R . \end{aligned} \tag{66}$$

For both points S' and R' situated in planes tangent to the wavefronts at S and R, respectively, we obtain

$$T(R', S') = T(R, S) + \tfrac{1}{2} q_M^R \big(\mathbf{P}_2^{(q)} \mathbf{Q}_2^{(q)-1}\big)_{MN} q_N^R + \tfrac{1}{2} q_M^S \big(\mathbf{Q}_2^{(q)-1} \mathbf{Q}_1^{(q)}\big)_{MN} q_N^S - q_M^S \big(\mathbf{Q}_2^{(q)-1}\big)_{MN} q_N^R \,. \tag{67}$$

Relation (67), of course, fully coincides with (27).

Specification of (47) for this case is simple. If the point S' is situated in the plane tangent to the wavefront at the point S, then due to the first equation of (63), eq. (47) yields

$$T(R', S') = T(R, S) + \delta x_i^R p_i(R) - \tfrac{1}{2} T^{-1}(R, S) \big[p_j(R) \delta x_j^R\big]^2 + \tfrac{1}{2} \delta x_i^R \big(\mathbf{P}_2^{(x)} \mathbf{Q}_2^{(x)-1}\big)_{ij} \delta x_j^R + \tfrac{1}{2} \delta x_i^S \big(\mathbf{Q}_2^{(x)-1} \mathbf{Q}_1^{(x)}\big)_{ij} \delta x_j^S - \delta x_i^S \big(\mathbf{Q}_2^{(x)-1}\big)_{ij} \delta x_j^R \,. \tag{68}$$

Analogously, we can obtain the expression for $T(R', S')$ if the point R' is situated in the plane tangent to the wavefront at the point R.

6.5 Points S' and/or R' on lines tangent to Ω at S and/or R

Consider point S' situated on the line tangent to the ray Ω at S. Then $\delta x_i^S f_{Mi}^S = 0$ as the vectors $\mathbf{f}_M^S$ are perpendicular to Ω at S, and (42) yields

$$T(R', S') = T(R, S) + \delta x_i^R p_i(R) - \delta x_i^S p_i(S) + \tfrac{1}{2} \delta x_i^R \big(F_{ij}^{RR} + \Phi_{ij}(R)\big) \delta x_j^R - \tfrac{1}{2} \delta x_i^S \Phi_{ij}(S) \delta x_j^S \,. \tag{69}$$

Analogously, we obtain for R' situated on the line tangent to the ray Ω at R, $\delta x_i^R f_{Mi}^R = 0$ and (42) reduces to

$$T(R', S') = T(R, S) + \delta x_i^R p_i(R) - \delta x_i^S p_i(S) + \tfrac{1}{2} \delta x_i^R \Phi_{ij}(R) \delta x_j^R + \tfrac{1}{2} \delta x_i^S \big(F_{ij}^{SS} - \Phi_{ij}(S)\big) \delta x_j^S \,. \tag{70}$$

Finally, if both points, S' and R' are situated on lines tangent to Ω at S and R, respectively, (42) reduces to

$$T(R', S') = T(R, S) + \delta x_i^R p_i(R) - \delta x_i^S p_i(S) + \tfrac{1}{2} \delta x_i^R \Phi_{ij}(R) \delta x_j^R - \tfrac{1}{2} \delta x_i^S \Phi_{ij}(S) \delta x_j^S \,. \tag{71}$$

As we can see from (71), the computation of $T(R', S')$ does not require solution of dynamic ray tracing along the reference ray from S to R and evaluation of the ray propagator matrix $\mathbf{\Pi}^{(q)}(R, S)$. Eq. (71) may be useful if we wish to extend moderately the reference ray and to compute traveltime along it. A straightforward application is the phenomenon of 'overshooting' in Fresnel volumes computations, see Section 7.4. The expression (47) does not simplify in this case.

6.6 Inhomogeneous isotropic media

In inhomogeneous isotropic media, computations of the two-point paraxial traveltime $T(R', S')$ and of the paraxial slowness vectors $\mathbf{p}(R')$ and $\mathbf{p}(S')$ is, of course, simpler than in inhomogeneous anisotropic media. First, the ray tracing and dynamic ray tracing equations are simpler. They are not presented here, as they are well known from literature. Secondly, we can take into account that the ray-velocity vector $\boldsymbol{\mathcal{U}}$ is parallel to the slowness vector $\mathbf{p}$:

$$\boldsymbol{\mathcal{U}} = v^2 \mathbf{p} \,, \quad \mathcal{U}_I^{(q)} = 0 \,, \tag{72}$$

where v is the velocity of P or S waves. Eq. (12) then yields for $\mathbf{f}_I$:

$$\mathbf{f}_1 = \mathbf{e}_1 \,, \quad \mathbf{f}_2 = \mathbf{e}_2 \,. \tag{73}$$

Expressions (41) thus take the form

$$F_{ij}^{RR} = e_{Mi}^R \big(\mathbf{P}_2^{(q)} \mathbf{Q}_2^{(q)-1}\big)_{MN} e_{Nj}^R \,, \quad F_{ij}^{SS} = e_{Mi}^S \big(\mathbf{Q}_2^{(q)-1} \mathbf{Q}_1^{(q)}\big)_{MN} e_{Nj}^S \,, \quad F_{ij}^{SR} = e_{Mi}^S \big(\mathbf{Q}_2^{(q)-1}\big)_{MN} e_{Nj}^R \,, \tag{74}$$

and vector $\boldsymbol{\eta}$ is given by the relation

$$\eta_i = -v^{-1} \partial v / \partial x_i \,. \tag{75}$$

Eqs (42) with (74) and (75) represent the two-point paraxial traveltime formula for inhomogeneous isotropic media.

The expression (47) remains formally the same even for an isotropic medium, only ray tracing and dynamic ray tracing equations simplify.

6.7 Homogeneous isotropic media

We can start from the expression for the two-point paraxial traveltime for a homogeneous anisotropic medium, eq. (50). Explicit expression for the 2×2 matrix $\mathbf{Q}_2^{(q)}$ for a homogeneous isotropic medium can be found in Červený (2001, eq. 4.8.3):

$$\mathbf{Q}_2^{(q)}(R, S) = v^2 T(R, S) \mathbf{I} \,. \tag{76}$$

If we take into account that $\mathbf{p}(R) = \mathbf{p}(S)$ and $\mathbf{f}_M^R = \mathbf{f}_M^S$, and an obvious relation $f_{Mi} f_{Mj} = \delta_{ij} - v^{-2} p_i p_j$, and insert all into eq. (50), we obtain

$$T(R', S') = T(R, S) + p_i(S) \big(\delta x_i^R - \delta x_i^S\big) + \tfrac{1}{2} T^{-1}(R, S) \big(\delta_{ij} v^{-2} - p_i p_j\big) \big(\delta x_i^R - \delta x_i^S\big) \big(\delta x_j^R - \delta x_j^S\big) \,. \tag{77}$$

Neglecting the terms of the order higher than two in δx_i^S, δx_j^R, we get from (77) an interesting expression for the two-point paraxial traveltime squared:

$$T^2(R', S') = T^2(R, S) + 2T(R, S) p_i(S) \big(\delta x_i^R - \delta x_i^S\big) + v^{-2} \big(\delta x_i^R - \delta x_i^S\big) \big(\delta x_i^R - \delta x_i^S\big) \,. \tag{78}$$

It is easy to see that eq. (78) is exact and that there are no problems with it when $R \to S$. Eq. (78) is valid for arbitrary δx_i^R and δx_i^S. For similar results see Ursin (1982) and Gjøystdal *et al.* (1984).

7 APPLICATIONS

The methodology described has many useful applications in seismology and seismic exploration. A few examples of such applications are described in the following. For simplicity, we refer to applications of expressions for $T(R', S')$ and related paraxial slowness vectors. The ray Ω may be computed in a smoothly varying isotropic or anisotropic medium with smooth structural interfaces. It is assumed that there is no caustics at the point R and that R is not too close to S. In the figures accompanying this section, reference and paraxial rays are drawn, respectively, as solid and dashed black curves.

7.1 Reflection times

We consider typical scenarios in reflection seismics where sources, S, and receivers, R, are situated on a measurement surface Σ. This surface Σ can be the Earth's surface, ocean bottom or some formal

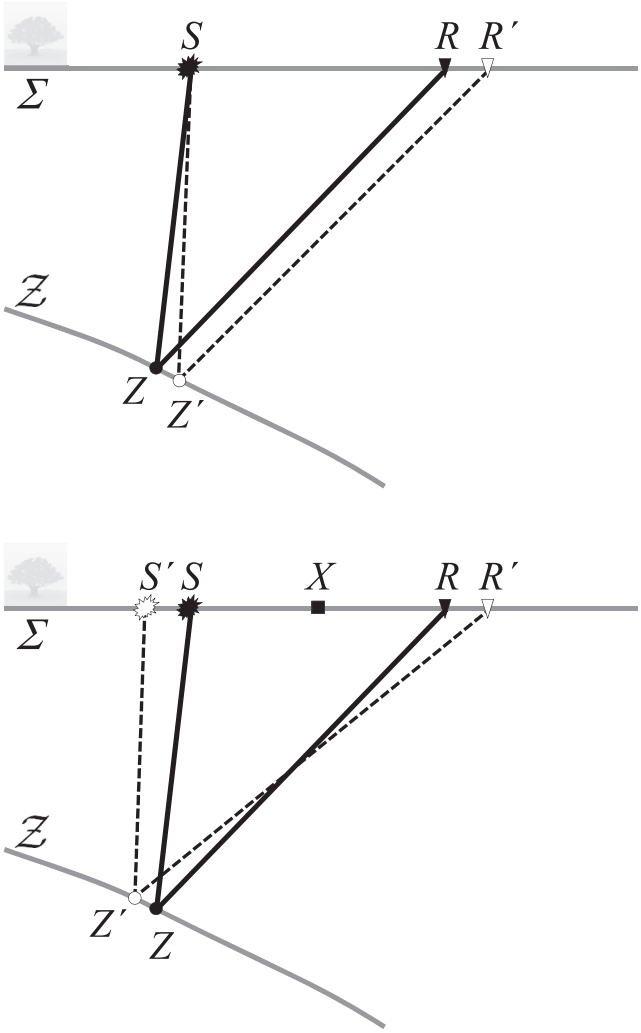

Figure 1. Reference (solid black) and paraxial (dashed black) reflected ray trajectories in common source (top) and common midpoint (bottom) situations.

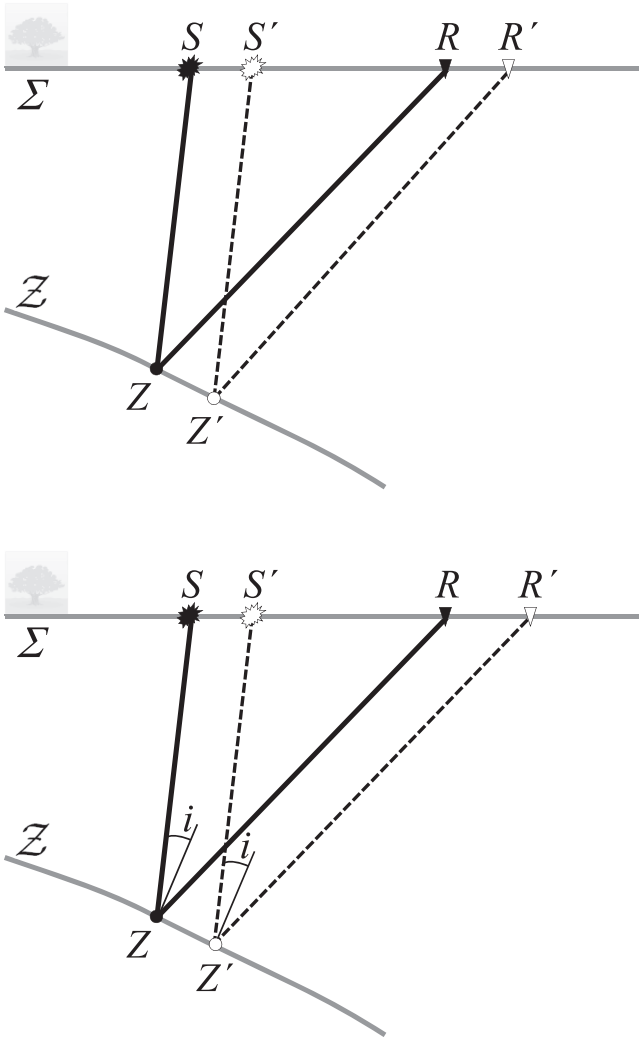

Figure 2. Reference (solid black) and paraxial (dashed black) reflected ray trajectories in common offset (top) and common angle of incidence (bottom) situations.

surface. At the measurement surface, we are recording reflections from a particular target reflector $\mathcal{Z}$. Such a reflection can be described by a reference ray from S to R via a reflection point Z on the reflector surface $\mathcal{Z}$. In many applications, it is useful to calculate reflection times by eqs (40) or (47) for source and receiver points S' and R' located at the surface Σ such that S' is close to S and R' is close to R. The corresponding reflection point Z' at the surface $\mathcal{Z}$ is assumed to be close to Z.

The upper plot of Fig. 1 depicts perhaps the most typical situation, namely common-source configuration, in which reference and paraxial rays start from the same point, that is, points S and S' coincide and points R and R' differ. Expressions from Section 6.2 can be used in this case. It is common in reflection seismics to sort or transform recorded traces into suitable data domains. In the bottom plot of Fig. 1, we illustrate the common midpoint configuration, in which reference and paraxial rays correspond to a common midpoint X between source and receiver. The upper plot in Fig. 2 shows the common-offset configuration, in which the distance vectors (or offset vectors) from S to R and S' to R' are identical. In a recently introduced imaging approach, 'common angle migration', the reference and paraxial rays have the same angle of incidence i. This is illustrated in the bottom plot of Fig. 2 for the 2-D situation. In the corresponding 3-D situation, one would need to require that the direction of incidence relative to the reflector normal, specified by the angle of incidence and one additional angle, say azimuth, is the same for the reference and paraxial rays. Alternatively, instead of considering the direction of incidence, projections of slowness vectors of incident wave upon the surface $\mathcal{Z}$ can be required equal for the reference and paraxial rays. In practice this can be achieved by dealing separately with the ray legs from Z' to S' and Z' to R'. In this case, from the given δx_i^Z and the condition that slowness vector projections along the reflector are the same everywhere, one can compute the changes of positions δx_i^S and δx_i^R. To determine the positions of S' and R', one can use results of the dynamic ray tracing along the reference rays from Z to S and from Z to R. Once the positions of S' and R' are known, it is possible to compute $T(S', Z')$ and $T(R', Z')$. For potential applications under the topic of common-angle migration, refer to, for example, Brandsberg-Dahl *et al.* (2003), Ursin (2004) and Koren & Ravve (2011).

7.2 CRS parameters

A CRS is a hypersurface for a particular reflection event described in four variables, for example, two variables for the source location and two variables for the receiver location. See more details in the following references describing 2-D and 3-D applications: Hubral *et al.* (1998), Jäger *et al.* (2001), Zhang *et al.* (2001) and Duveneck (2004). The most common way of representing the CRS is with respect to two offset coordinates and two midpoint coordinates. At zero offset the source S, receiver R and midpoint X locations coincide. For primary unconverted reflections, the ray legs from Z to S and Z to R also coincide. As a consequence, the corresponding two-way zero-offset reflections can be modelled using normal rays. These rays start at the reflector $\mathcal{Z}$ with slowness vector normal to $\mathcal{Z}$, and are continued in one direction (upwards) until they hit the measurement surface Σ (top of Fig. 3). The corresponding (hypothetical) wave is called the normal wave, which is closely tied to the exploding reflector concept (Claerbout 1985). Traveltimes from Z' to X' can be again estimated from expressions (40) or (47).

Let us take a normal ray as a reference ray, as in upper plot of Fig. 3. If the initial point Z is kept common for the reference and paraxial rays (bottom plot of Fig. 3), the system of paraxial rays in the vicinity of the reference normal ray describes the (hypothetical) so-called normal-incidence point wave (or NIP wave). In this situation, the (one-way) second-order coefficients of eqs (40) or (47) are directly related to (two-way) second-order reflection traveltime parameters that can be retrieved from observed seismic reflection traveltime data. In particular, the second-order coefficients for fixed Z (NIP wave situation) are connected with observed normal-moveout (NMO) velocity.

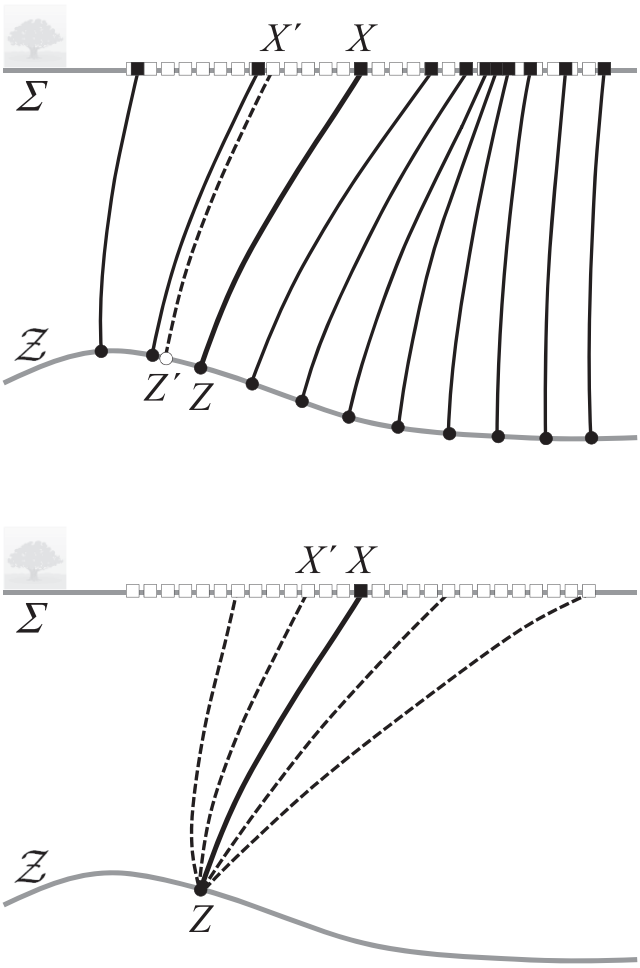

Figure 3. One-way reference (solid black) and paraxial (dashed black) ray trajectories from reflector to measurement surface: 'exploding reflector' ray field (top) and point-source ray field (bottom).

7.3 Green's function traveltimes

The Green's function plays a fundamental role in the theories of seismic wave propagation and seismic imaging. Moreover, quite often the ray-theoretical Green's function corresponding to an elementary wave (Červený 2001; Červený *et al.* 2007) is preferred to a complete wavefield Green's function as it is more efficiently computed and has explicit traveltimes. Such Green's function traveltimes are of great value in many modelling and imaging applications, in particular in those using Kirchhoff/Helmholtz type of integrals, see, for example Gjøystdal *et al.* (2007).

An illustration addressing Kirchhoff depth migration is depicted in the upper plot of Fig. 4. A typical situation is that the Green's function traveltimes $T(Z, S)$ and $T(Z, R)$ are calculated in an initial forward modelling operation using relatively course grids for the sources S, receivers R and image points Z. The initial modelling operation can, for example, be performed using the wavefront construction method (Vinje *et al.* 1993). Subsequently one may utilize eq. (40) or (47) to obtain paraxial traveltimes $T(Z', S')$ and $T(Z', R')$

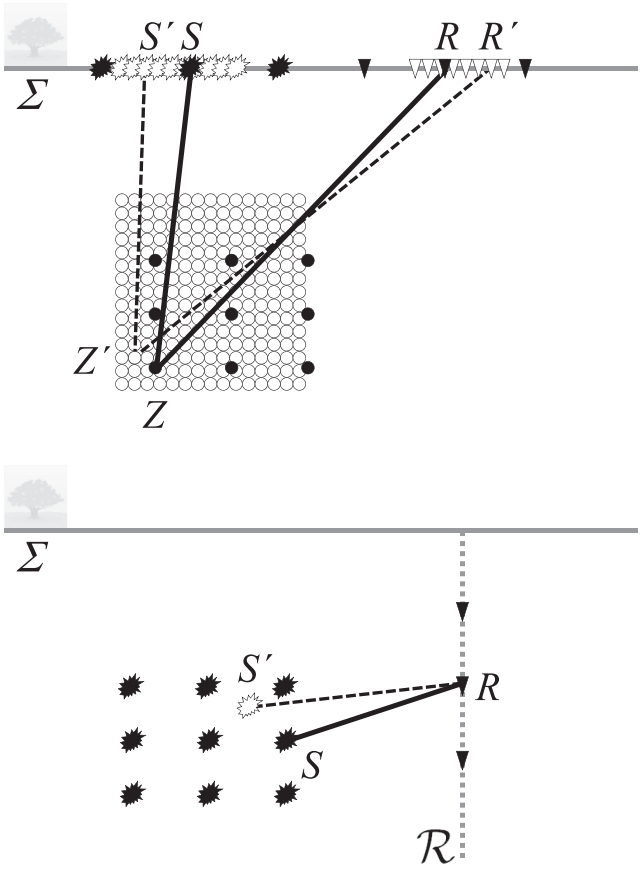

Figure 4. Application of Green's function paraxial traveltimes in Kirchhoff pre-stack depth migration (top) and microseismic monitoring (bottom).

of the wave with the same history (the same branch of the wave if there is multipathing) for a large number of locations S', R' and Z' situated on much denser grids than the original points S, R and Z. In this way, eqs (40) or (47) have enormous impact with respect to lowering the total computation time of Kirchhoff depth migration and other Kirchhoff type modelling/imaging approaches.

The bottom plot of Fig. 4 illustrates application of Green's function traveltimes in the context of microseismic monitoring, see, for example, Gharti *et al.* (2010). In this situation the problem under consideration is to estimate the source location S' of a microearthquake. The estimation is often based on receiver R recordings in a borehole $\mathcal{R}$ and pre-calculated traveltimes corresponding to a grid of potential source (S) locations. In this case, it might be preferable to use expressions (43) or (48) for the traveltime squared since they may be more accurate than (40) or (47) for short distances between sources and receivers.

7.4 Fresnel zones and volumes

One application of eqs (40) or (47) is an alternative way to estimate Fresnel zones or Fresnel volumes (Červený & Soares 1992) corresponding to a given reference ray. Fig. 5 illustrates this in the settings of global seismology (top panel) and reflection seismics (bottom panel). One particular application in reflection seismics is so-called Fresnel volume migration (Buske *et al.* 2009). Note that the two-point paraxial traveltime computations in Cartesian coordinates naturally account for the phenomenon of 'overshooting', that is, the extension of Fresnel volumes beyond the points S and R. This is an important feature of formulae presented in this paper because the procedure based on ray-centred coordinates only, without their transformation to Cartesian coordinates, leads to zero cross-sections of a Fresnel volume at S and R.

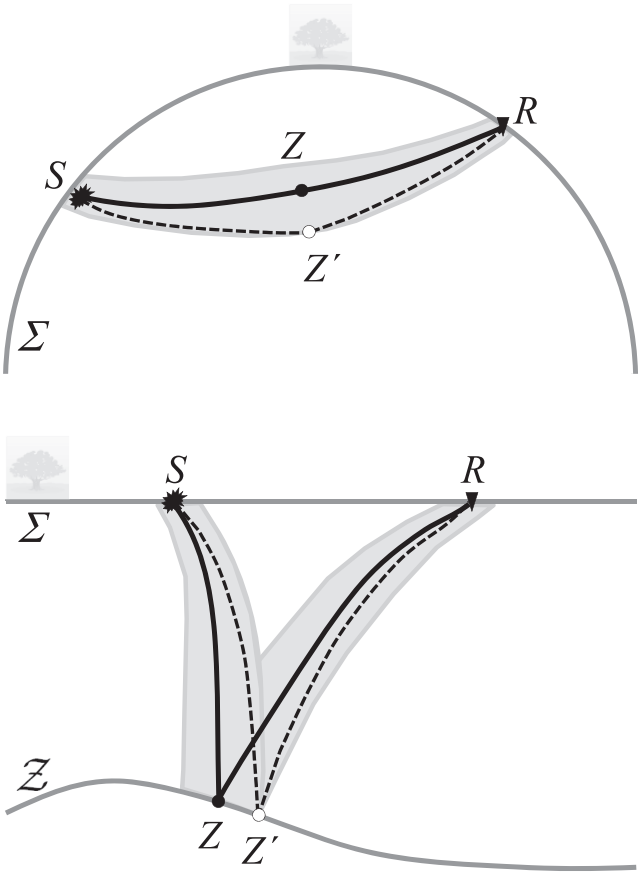

Figure 5. Fresnel zones and volumes for typical applications in global seismology (top) and reflection seismics (bottom).

8 CONCLUDING REMARKS

We presented expressions for the approximate computation of two-point paraxial traveltimes between points S' and R' arbitrarily chosen in a paraxial vicinity of points S and R on a reference ray Ω. The ray Ω may be be computed in a smoothly varying, layered isotropic or anisotropic medium. It is assumed that there is no caustics at R and that R is not close to S. In addition, we also offered expressions for paraxial slowness vectors, which specify paraxial rays connecting points S' and R'. All the expressions depend on quantities calculated during ray tracing and dynamic ray tracing in ray-centred coordinates. Alternatively, the dynamic ray tracing can be performed in Cartesian coordinates.

The expressions based on ray propagator matrices in ray-centred or directly in Cartesian coordinates can be used alternatively, but they have a different form and depend on different quantities. All depend on three submatrices of the ray propagator matrix, specifically on $\mathbf{Q}_1$, $\mathbf{Q}_2$ and $\mathbf{P}_2$. They do not depend on the submatrix $\mathbf{P}_1$. In Cartesian coordinates, the mentioned matrices are 3×3 and their evaluation requires computation of the 6×6 propagator matrix. It is well known that the 6×6 ray propagator matrix $\mathbf{\Pi}^{(x)}(R, S)$ in Cartesian coordinates includes the non-eikonal solutions of the dynamic ray tracing equations. From this reason, the equation for $T(R', S')$ derived in Section 5 contains terms, which are consequence of these solutions (Klimeš 2009); see the terms with $T^{-1}(R, S)$ in (46), also in (47). In contrast to this, the non-eikonal solutions play no role in derivations of the equation for $T(R', S')$ based on the 4×4 ray propagator matrix $\mathbf{\Pi}^{(q)}(R, S)$ in ray-centred coordinates in Section 4.

In addition to expressions for traveltime between paraxial points S' and R', we also presented expressions for its square. Squared traveltime plays a basic role in normal moveout studies (see, e.g. Tsvankin 2001). For results and applications of squared traveltime see also Ursin (1982) and Gjøystdal *et al.* (1984). The expressions for the traveltime squared in homogeneous isotropic media yield exact traveltimes. Thus, it is expected that the use of expressions for traveltime squared in weakly inhomogeneous media, either isotropic or weakly anisotropic, may provide highly accurate results. We further derived expressions for paraxial slowness vectors at points S' and R', both in Cartesian coordinates. These slowness vectors may be used as initial conditions for construction of exact ray trajectories (using standard ray tracing). Deviation of approximate and exact trajectories is an indicator of accuracy of paraxial ray tracing procedure. The obvious application of approximate ray trajectory computations is in tomography. Attempts are made to derive procedure for an approximate computation of ray amplitudes related to two-point paraxial traveltimes.

In this paper, we concentrated on the evaluation of traveltime between two paraxial points located in a vicinity of a single (there is no need for considering a ray field) reference ray and to determination of slowness vectors at the paraxial points. Explicit knowledge of paraxial rays (rays in a vicinity of the reference ray) was not required. It would be possible to extend this study and to also

evaluate the paraxial rays, which would allow to make the experiment shown in the bottom part of Fig. 2. Besides several practical applications, it would allow us to also consider common *S*-wave rays, which are important entities in studies of *S*-wave propagation in inhomogeneous, weakly anisotropic media.

Estimate of errors of two-point paraxial traveltime formula is a complicated problem. It is a problem of the paraxial ray method and the ray method as a whole. There were many attempts to solve this problems, but so far, they did not lead to satisfactory results. In principle, there are two approaches to its solution. One requires computation of third spatial partial derivatives of traveltime along the reference ray. This would allow estimation of accuracy of the second-order expansion of traveltime into the Taylor series. Computation of third spatial derivatives of traveltime, however, requires model derivatives smooth up to the third order (Klimeš 2002). Thus, at present broadly used cubic spline approximation would not be sufficient, higher-order spline approximation would be required. We are afraid that such procedures would not be useful in applications. The other approach how to estimate accuracy of two-point paraxial traveltimes is to compare the results of the equation proposed in this paper with exactly computed traveltimes. We are working on such a comparison. It will be a subject of the follow-up paper, in which we also show a simple way of enhancing accuracy by using the Shanks transform (Bender & Orszag 1978).

A useful by-product of two-point paraxial traveltime computations are ray amplitudes, which can be evaluated along the reference ray from quantities obtained from the dynamic ray tracing. Computation of paraxial ray amplitudes, that is, computation of the ray amplitudes along paraxial rays, is, however, a considerably more complicated problem than computation of ray amplitudes along the reference ray. Similarly as the error estimates discussed in the previous paragraph, computation of paraxial amplitudes would require spatial derivatives of the model parameters of orders higher than second. Relevant algorithms have not yet be proposed and their usefulness for practical applications is questionable.

Finally, let us emphasize that the two-point paraxial traveltime formula proposed in this paper is based on the 'single ray approach'. This means that the formula is useful for the determination of traveltimes between points in a vicinity of a single reference ray, not for an interpolation of traveltimes between rays used, for example by Vinje *et al.* (1993) or Bulant & Klimeš (1999).

ACKNOWLEDGMENTS

The authors are greatly indebted to Luděk Klimeš for helpful suggestions and valuable discussions. Referees' comments and suggestions are highly appreciated. The research has been supported by the Grant Agency of the Czech Republic under the contracts P210/10/0736 and P210/11/0117, by the Ministry of Education of the Czech Republic within Research Project MSM0021620860, and by the Consortium 'Seismic Waves in Complex 3-D Structures'. EI acknowledges support from the Research Council of Norway via NORSAR's project 194064/I30 and from the European Community's FP7 Consortium Project AIM 'Advanced Industrial Microseismic Monitoring', Grant Agreement No. 230669.

REFERENCES

Alkhalifah, T. & Fomel, S., 2010. An eikonal-based formulation for traveltime perturbation with respect to the source location, *Geophysics,* **75,** T175–T183.

Arnaud, J.A., 1971. Mode coupling in first-order optics, *J. Opt. Soc. Am.,* **61,** 751–758.

Babich, V.M., 1961. Ray method of the computation of the intensity of wave fronts in elastic inhomogeneous anisotropic medium, in *Problems of the Dynamic Theory of Propagation of Seismic Waves* (in Russian), Vol. 5, pp. 36–46, ed. Petrashen, G.I., Leningrad University Press, Leningrad. [Translation to English: *Geophys. J. Int.,* **118,** 379–383, 1994.]

Bender, C.M. & Orszag, S.A., 1978. *Advanced Mathematical Methods for Scientists and Engineers,* McGraw-Hill, Singapore.

Bortfeld, R., 1989. Geometrical ray theory: rays and traveltimes in seismic systems (second-order approximation of the traveltimes), *Geophysics,* **54,** 342–349.

Brandsberg-Dahl, S., de Hoop, M.V. & Ursin, B., 2003. Focusing in dip and AVA compensation on scattering-angle/azimuth common image gathers, *Geophysics,* **68,** 232–254.

Bulant, P., 1996. Two-point ray tracing in 3-D, *Pageoph,* **148,** 421–448.

Bulant, P., 1999. Two-point ray tracing and controlled initial-value ray tracing in 3-D heterogeneous block structures, *J. seism. Explor.,* **8,** 57–75.

Bulant, P. & Klimeš, L., 1999. Interpolation of ray theory traveltimes within ray cells, *Geophys. J. Int.,* **139,** 273–282.

Buske, S., Gutjahr, S. & Sick, Ch., 2009. Fresnel volume migration of single-component seismic data, *Geophysics,* **74,** WCA47–WCA55.

Chapman, C.H., 2004. *Fundamentals of Seismic Wave Propagation,* Cambridge University Press, Cambridge.

Červený, V., 1972. Seismic rays and ray intensities in inhomogeneous anisotropic media, *Geophys. J.R. astr. Soc.,* **29,** 1–13.

Červený, V., 2001. *Seismic Ray Theory,* Cambridge University Press, Cambridge.

Červený, V. & Klimeš, L., 2010. Transformation relations for second order derivatives of travel time in anisotropic media, *Stud. geophys. Geod.,* **54,** 257–267.

Červený, V. & Moser, T.J., 2007. Ray propagator matrices in three-dimensional anisotropic inhomogeneous layered media, *Geophys. J. Int.,* **168,** 593–604.

Červený, V. & Soares, J.E.P., 1992. Fresnel volume ray tracing, *Geophysics,* **57,** 902–915.

Červený, V., Klimeš, L. & Pšenčík, I., 1984. Paraxial ray approximations in the computation of seismic wavefields in inhomogeneous media, *Geophys. J.R. astr. Soc.,* **79,** 89–104.

Červený, V., Klimeš, L. & Pšenčík, I., 2007. Seismic ray method: recent developments, *Adv. Geophys.,* **48,** 1–126.

Claerbout, J.F., 1985, *Imaging the Earth's Interior,* Blackwell, Oxford.

Duveneck, E., 2004. 3D tomographic velocity model estimation with kinematic wavefield attributes, *Geophys. Prospect.,* **52,** 535–545.

Farra, V. & LeBégat, S., 1995. Sensitivity of qP-wave traveltimes and polarization vectors to heterogeneity, anisotropy and interfaces, *Geophys. J. Int.,* **121,** 371–384.

Farra, V. & Madariaga, R., 1987. Seismic waveform modeling in heterogeneous media by ray perturbation theory, *J. geophys. Res.,* **92**(B3), 2697–2712.

Gajewski, D. & Pšenčík, I., 1987. Computation of high-frequency seismic wavefield in 3-D laterally inhomogeneous anisotropic media, *Geophys. J. R. astr. Soc.,* **91,** 383–411.

Gajewski, D. & Pšenčík, I., 1990. Vertical seismic profile synthetics by dynamic ray tracing in laterally varying layered anisotropic structures, *J. geophys. Res.,* **95,** 11 301–11 315.

Gharti, H.N., Oye, V., Roth, M. & Kühn, D., 2010. Automated microearthquake location using envelope stacking and robust global optimization, *Geophysics,* **75,** MA27–MA46.

Gjøystdal, H., Reinhardsen, I.E. & Ursin, B., 1984. Traveltime and wavefront curvature calculations in three-dimensional inhomogeneous layered media with curved interfaces, *Geophysics,* **49,** 1466–1494.

Gjøystdal, H., Iversen, E., Lecomte, I., Kaschwich, T., Drottning, A. & Mispel, J., 2007. Improved applicability of ray tracing in seismic acquisition, imaging, and interpretation, *Geophysics,* **72,** SM261–SM271.

Grechka, V.J. & McMechan, G.A., 1996. 3-D two-point ray tracing for heterogeneous weakly transversely isotropic media, *Geophysics,* **61,** 1883–1894.

Hamilton, W.R., 1837. Third supplement to an essay on the theory of systems of rays, *Trans. Roy. Irish Acad.,* **17,** 1–144.

Hubral, P., Schleicher, J. & Tygel, M., 1992. Three-dimensional paraxial ray properties. Part I. Basic relations, *J. seism. Explor.,* **1,** 265–279. [Part II. Applications, *J. seism. Explor.,* **1,** 347–362.]

Hubral, P., Höcht, G. & Jäger, R., 1998. An introduction to the Common Reflection Surface stack. In *Proceedings of the 60st Annual Int. Meeting, EAGE, Expanded Abstracts,* session 1-19, Houston.

Iversen, E., 2004. Reformulated kinematic and dynamic ray tracing systems for arbitrary anisotropic media, *Stud. geophys. Geod.,* **48,** 1–20.

Jäger, R., Mann, J., Höcht, G. & Hubral, P., 2001. Common-reflection-surface stack: image and attributes, *Geophysics,* **66,** 97–109.

Klimeš, L., 1994. Transformations for dynamic ray tracing in anisotropic media, *Wave Motion,* **20,** 261–272.

Klimeš, L., 2002. Second-order and higher-order perturbations of travel time in isotropic and anisotropic media, *Stud. geophys. Geod.,* **46,** 213–248.

Klimeš, L., 2006a. Ray-centred coordinate systems in anisotropic media, *Stud. geophys. Geod.,* **50,** 431–447.

Klimeš, L., 2006b. Common-ray tracing and dynamic ray tracing for S waves in a smooth elastic anisotropic medium, *Stud. geophys. Geod.,* **50,** 449–461.

Klimeš, L., 2009. Relation between the propagator matrix of geodesic deviation and second-order derivation of characteristic function, in *Seismic Waves in Complex 3-D Structures, Report 19,* pp. 103–114, Faculty of Mathematics and Physics, Department of Geophysics, Charles University, Prague. [Available at: http: //sw3d.cz.]

Koren, Z. & Ravve, I., 2011. Full-azimuth subsurface angle domain wavefield decomposition and imaging, Part I: directional and reflection image gathers, *Geophysics,* **76,** S1–S13.

Luneburg, R.K., 1964. *Mathematical Theory of Optics,* University of California Press, Berkeley, CA, USA.

Moser, T.J. & Červený, V., 2007. Paraxial ray methods for anisotropic inhomogeneous media, *Geophys. Prospect.,* **55,** 21–37.

Schleicher, J., Tygel, M. & Hubral, P., 1993. Parabolic and hyperbolic 2-point travel-times in 3D media, *Geophys. Prospect.,* **41,** 495–513.

Tsvankin, I., 2001. *Seismic Signatures and Analysis of Reflection Data in Anisotropic Media,* Elsevier Science Ltd., Oxford, UK.

Ursin, B., 1982. Quadratic wavefront and travel time approximations in inhomogeneous layered media with curved interfaces, *Geophysics,* **47,** 1012–1021.

Ursin, B., 2004. Parameter inversion and angle migration in anisotropic elastic media, *Geophysics,* **69,** 1125–1142.

Vinje, V., Iversen, E. & Gjøystdal, H., 1993. Traveltime and amplitude estimation using wavefront construction, *Geophysics,* **58,** 1157–1166.

Zhang, Y., Bergler, S. & Hubral, P., 2001. Common-reflection-surface (CRS) stack for common offset. *Geophys. Prospect.,* **49,** 709–718.